Operational Experience and Performance with the ATLAS Pixel detector at the Large Hadron Collider at CERN

VERTEX 2022, Tateyama Resort Hotel, 24-10-2022

Kerstin Lantzsch

universitätbonn

Introduction

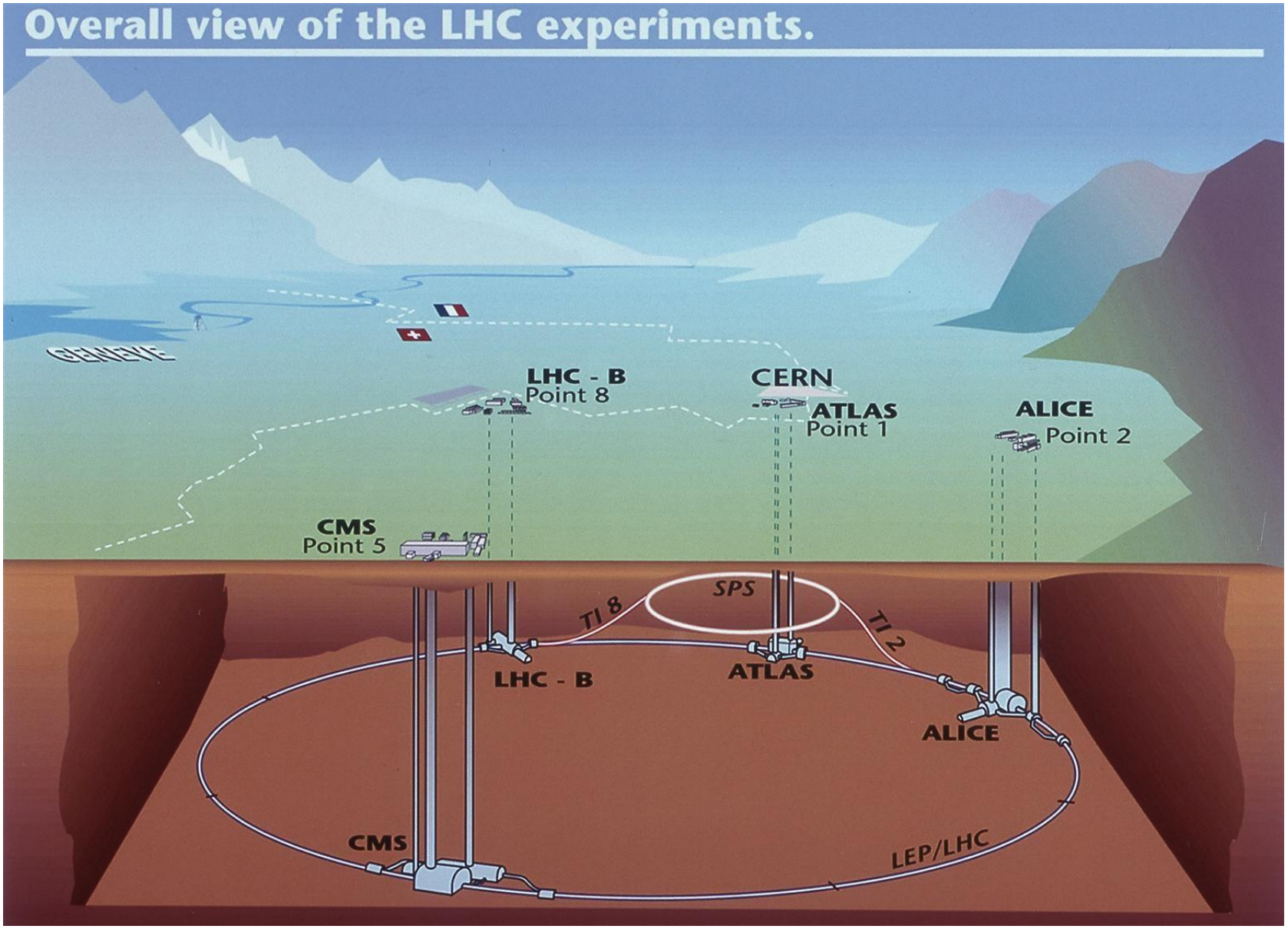

LHC

The Large Hadron Collider

Introduction

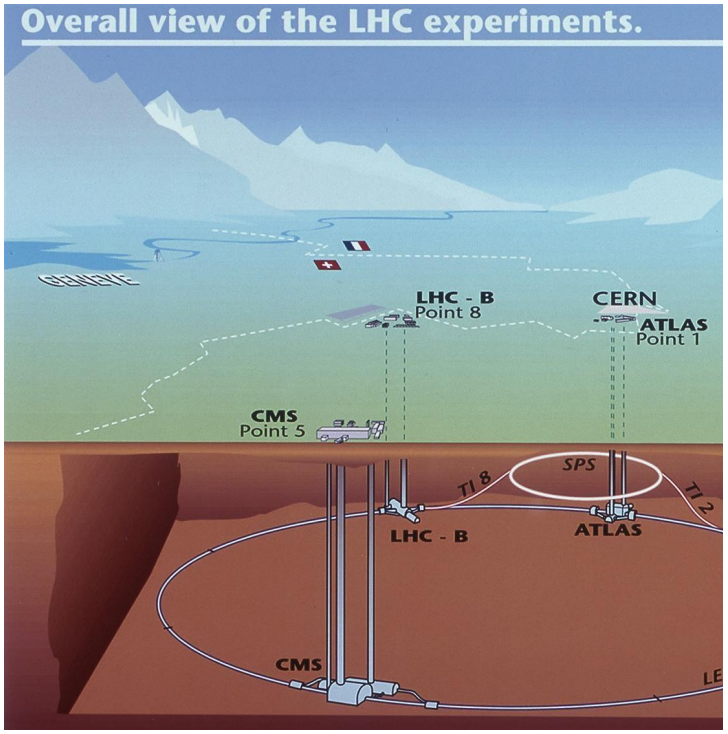

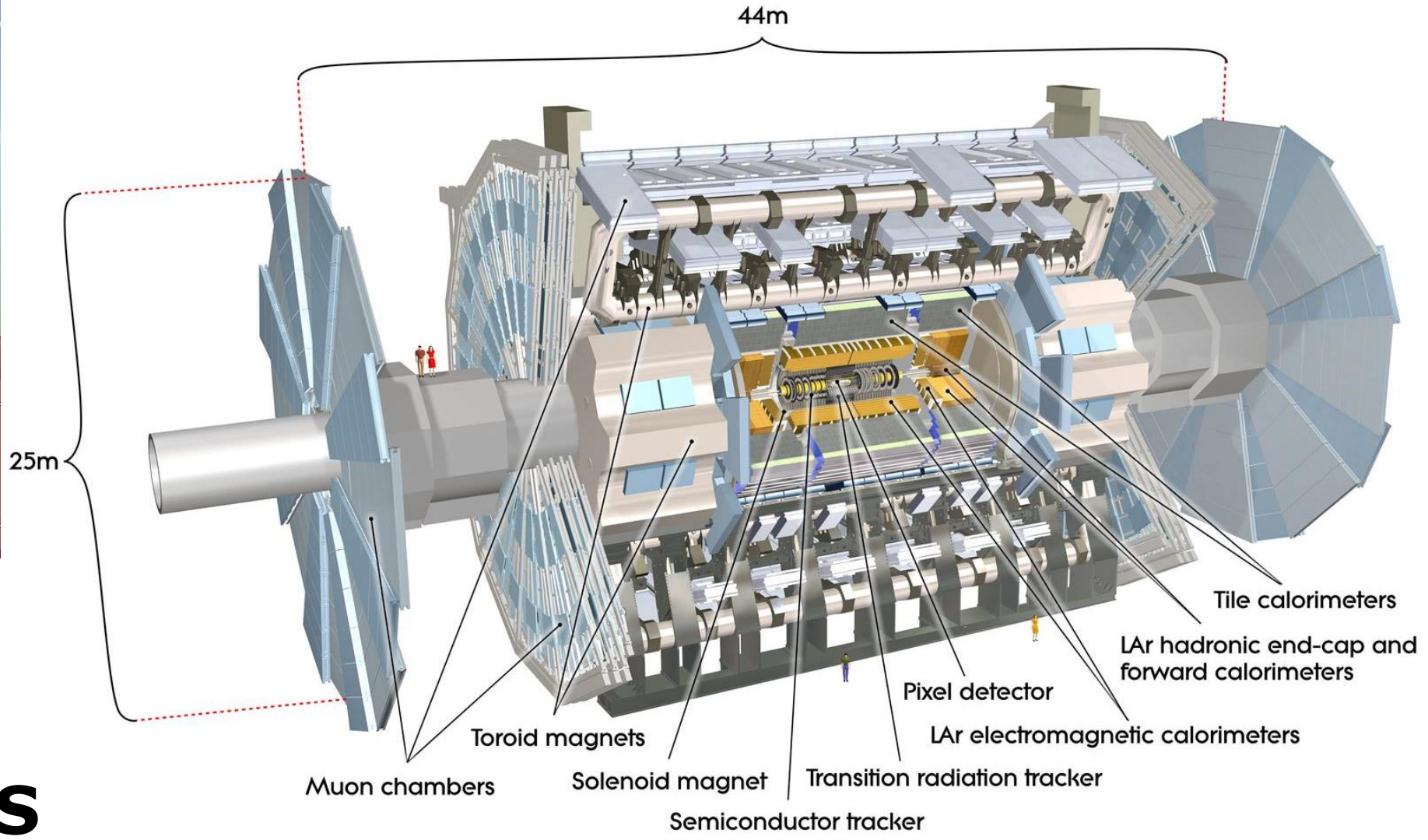

ATLAS

A Toroidal LHC Apparatus

Introduction

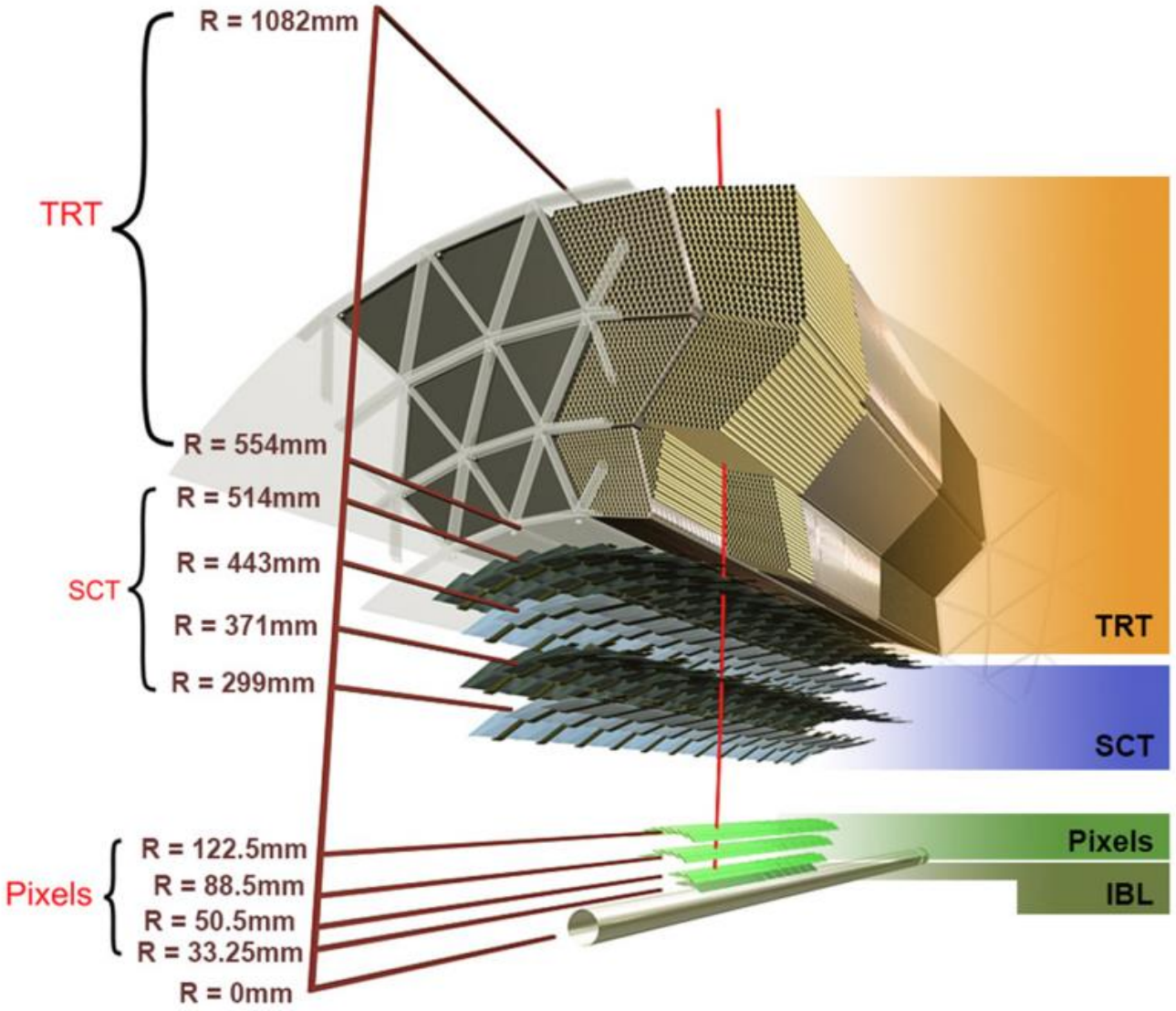

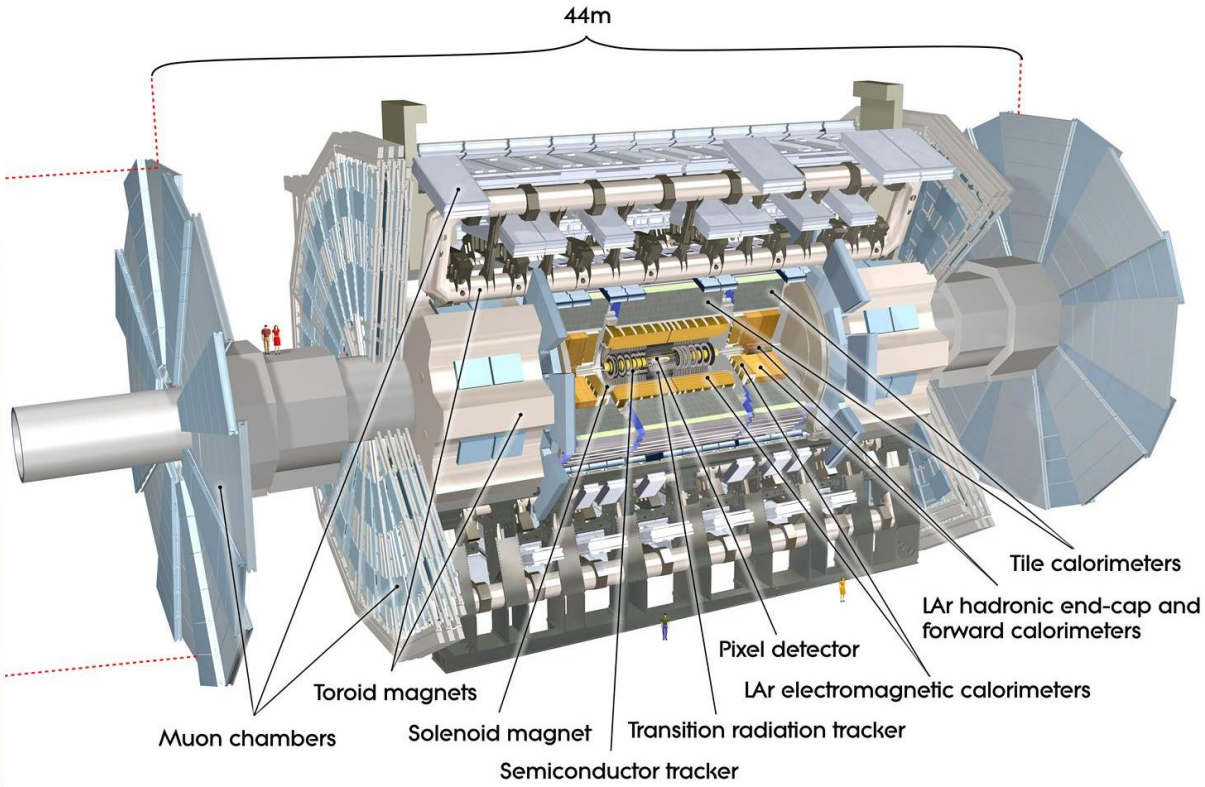

The

ATLAS PIXEL DETECTOR

LHC Run 3

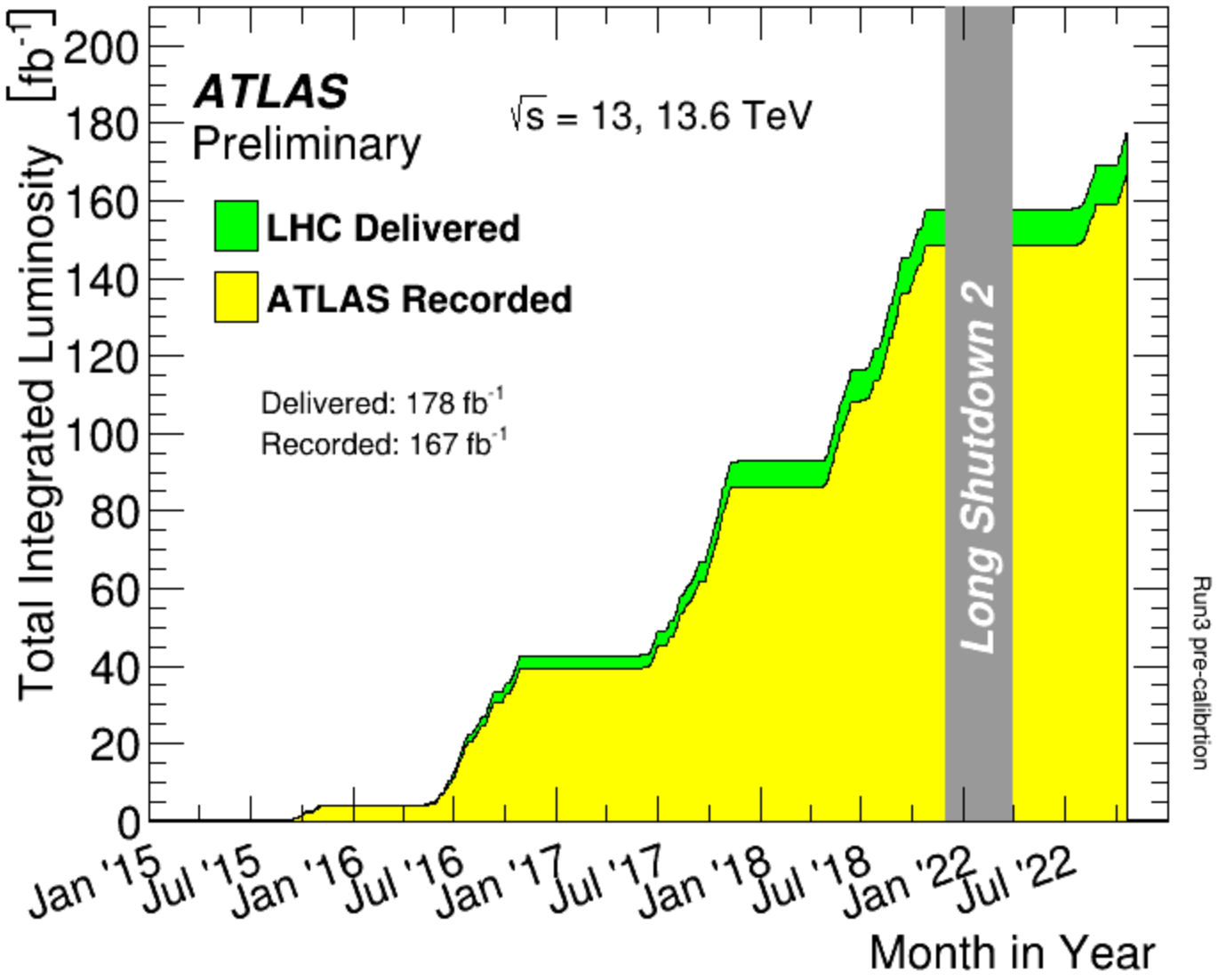

LHC Run 3

- Restart in 2022 after three years of shutdown:
  - Long Shutdown 2 (LS2) from 2019 – 2021
- Unprecedented energy of 13.6 TeV
- Instantaneous luminosity 2×10^{34} cm^2/s
  - Peak average pileup in ATLAS of ~52 - 55 (levelled)
- Collected this year up to now ca 20 fb^{-1}.
  - End of 2022 running: November 28th.
- Predictions for Run 3: collect 200-300 fb^{-1}.

LHC Run 3

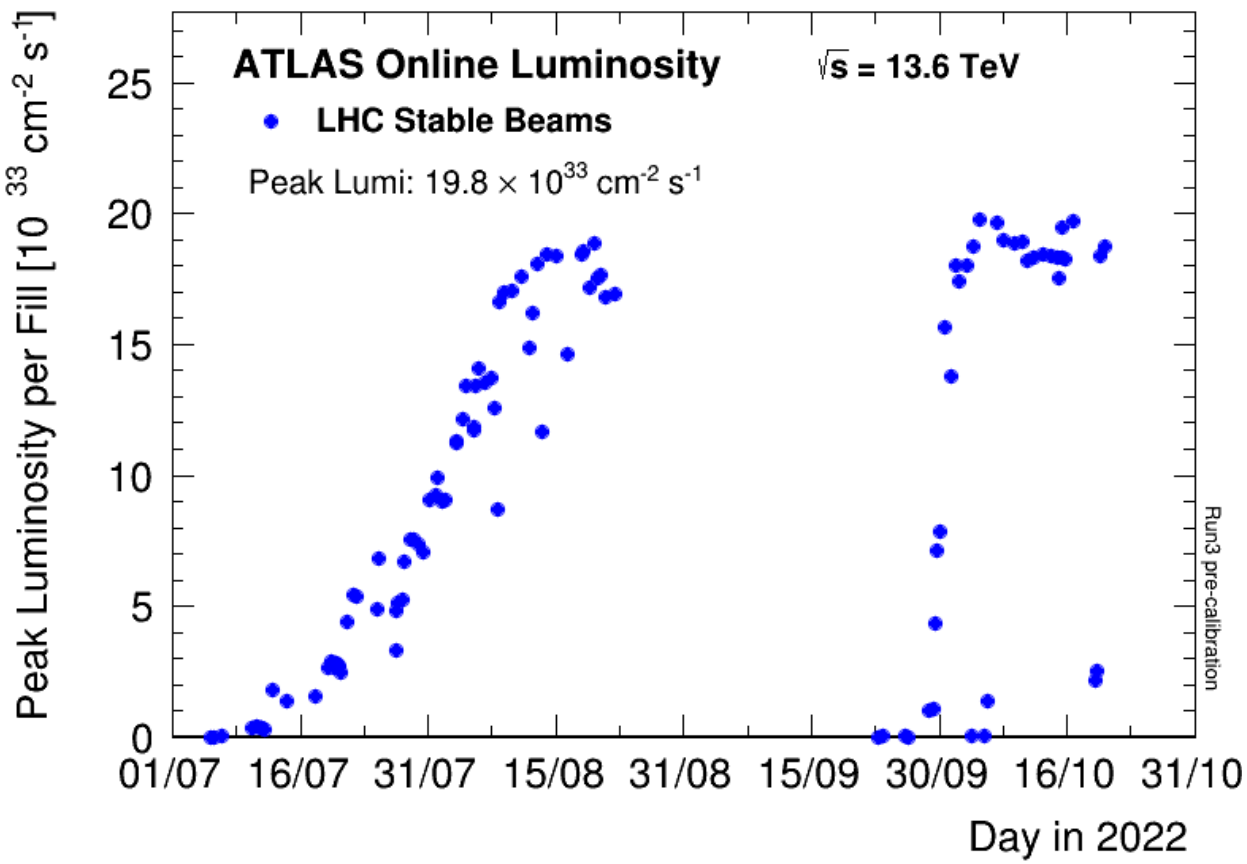
ATLAS Online Luminosity
√s = 13.6 TeV
LHC Stable Beams
Peak Lumi: 19.8 × 10^33 cm^-2 s^-1
Peak Luminosity per Fill [10^33 cm^-2 s^-1]
Day in 2022
Run3 pre-calibration

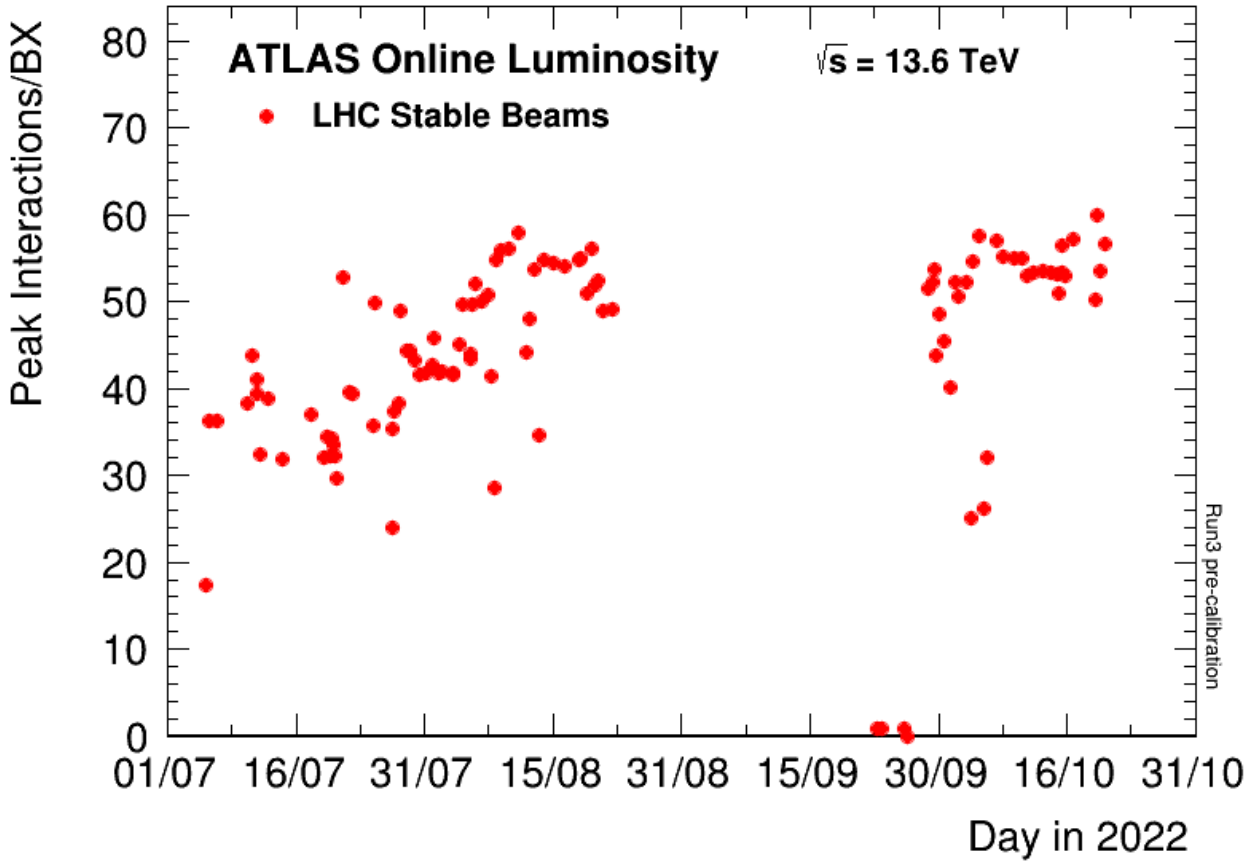
ATLAS Online Luminosity
√s = 13.6 TeV
LHC Stable Beams
Peak Interactions/BX
Day in 2022
Run3 pre-calibration

The Pixel Detector

- 1.7 m^2 of silicon, 80 million channels, 1744 modules.
- Three barrel layers and 2x3 endcap disks.
  - Radius of 5.05 cm, 8.85 cm, 12.25 cm of B-Layer, Layer 1, Layer 2.
- Angular coverage |eta| < 2.5
- C_3F_8 evaporative cooling system.

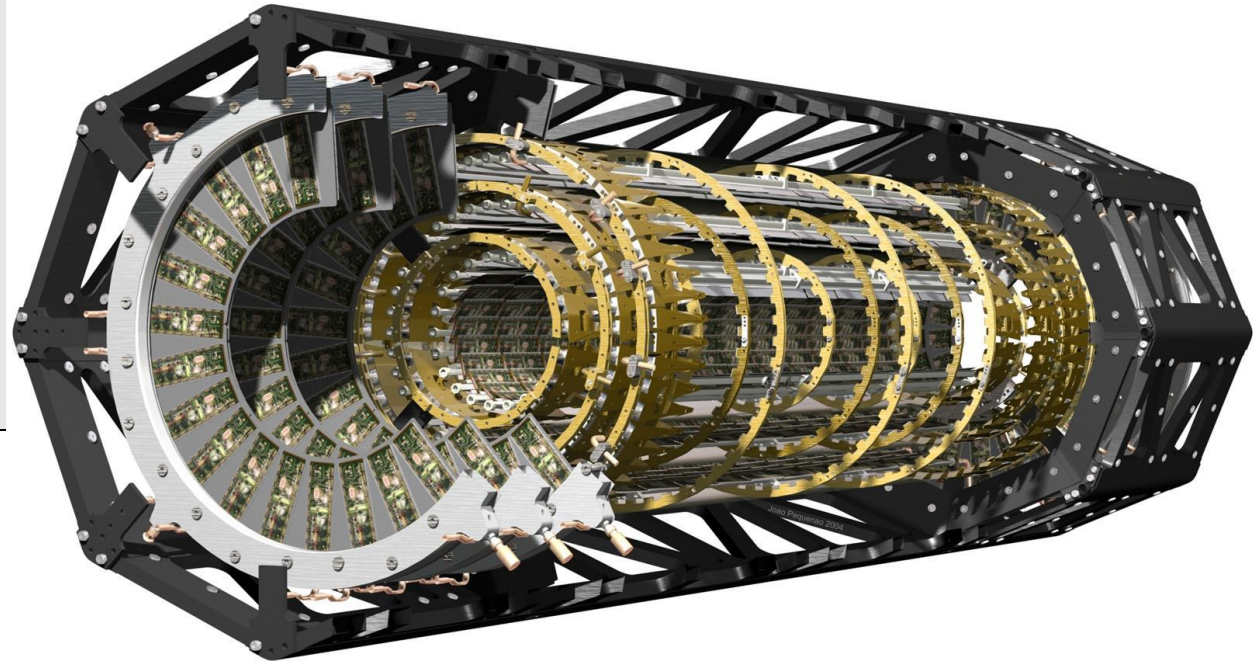

- Sensor: planar n^+-in-n sensor, 60.8 mm x 16.4 mm active area, 250 µm thick.
- 16 FE-I3 frontend chips plus one controller (MCC) in 0.25 µm CMOS technology.
- The frontends are bump-bonded to the sensors with solder and indium bumps.
- Radiation hard to 1 x 10^{15} neq/cm^2.

- 46'080 Pixels per module.
- 10 x 115 µm resolution.
- Pixel size: 50 µm x 400 µm.
- 8-bit Time-over-threshold information per hit.

The Insertable B-Layer (IBL)

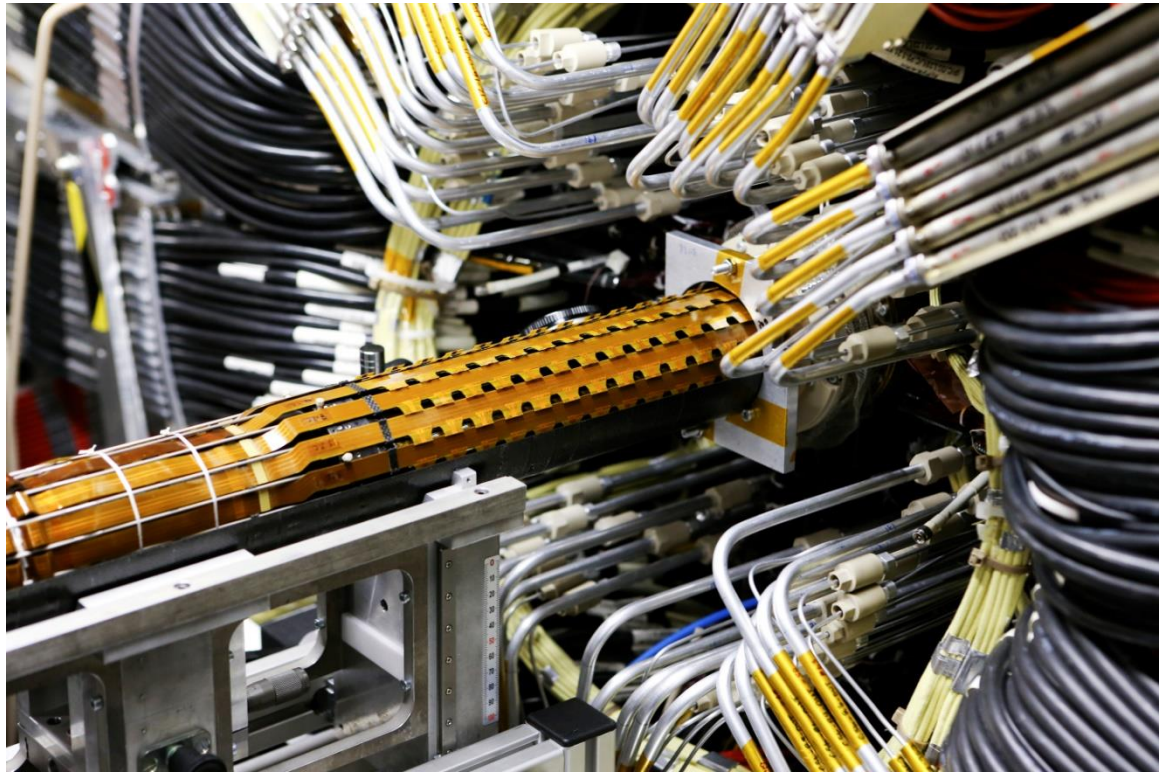

- New innermost layer of the Pixel Detector, **added in the 2013-2014 LHC shutdown (LS1)**.
- 14 staves at a radius of 3.2 cm in a radial envelope of 9 mm.
- CO_2 evaporative cooling, 2 redundant plants.

- 0.2 m^2 of silicon
- 12 million channels
- 280 modules
- Two sensor types:
  - planar n^+-in-n, 200 µm thick
  - 3D n^+-in-p sensors,230 µm thick, at high eta.
- Radiation hard to 5 x 10^{15} neq/cm^2.

3D

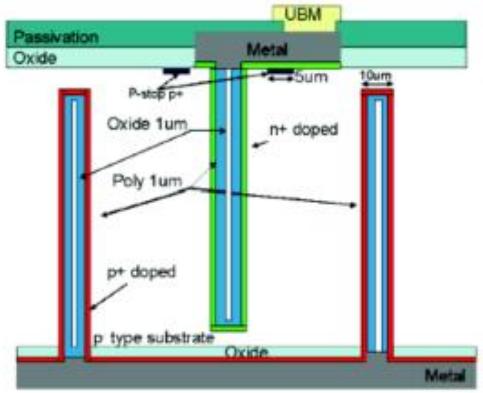

- 448 FE-I4 frontends, 130 nm CMOS technology
  - two per planar sensor, and one per 3D sensor, solder-bump-bonded.
- Size: 2 cm x 1.8 cm, 26’880 pixels per fronted.
- 4-bit Time-over-threshold information per hit.

New Service Quarter Panels

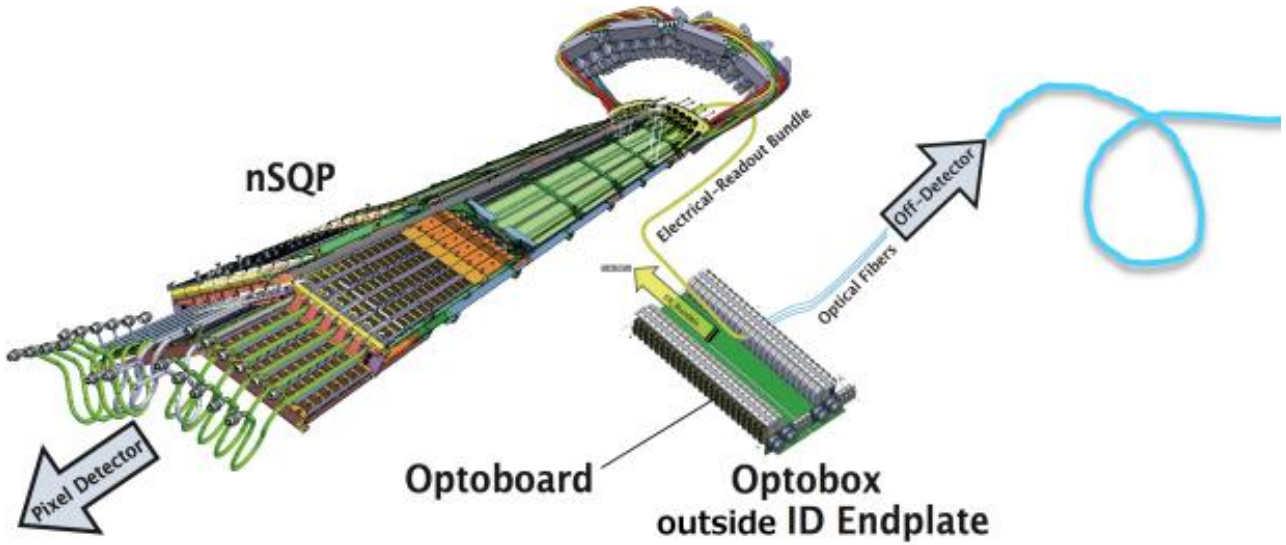

On-detector

Optical Fiber
70-90 m

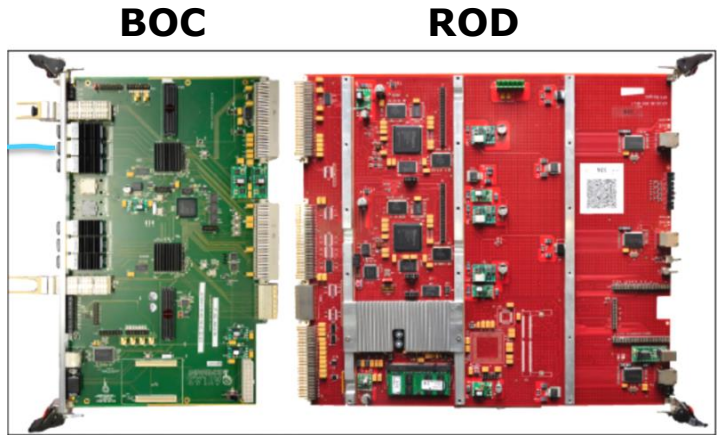

Off-detector

- In LS1 (2013-2015), the new Service Quarter Panels (nSQPs) were installed into the detector.
  - Reproduction of the old Pixel service panels, but with the optoboards outside the detector volume, in an accessible region.
  - Double the amount of readout lines for Layer 1 to cope with the expected bandwidth in Run 2. To exploit this upgrade, the off-detector readout was unified between Pixel and IBL during the course of Run 2.

Operation in Run 2: Bandwidth

- Bandwidth considerations: Hit Occupancy (and event size) scales with pileup, level 1 trigger rate depends on instantaneous luminosity.
- For Pixel, both luminosity and pileup are much higher than originally specified.
- High occupancy can lead to buffer overflows resulting in event fragments being associated with the wrong event (“desynchronization”).
- A **periodic reset** of the frontend ASICs and of the firmware in the backend every 5 seconds was introduced to resynchronize all data sources.
- In 2018, the fraction of desynchronization was less than 1%.

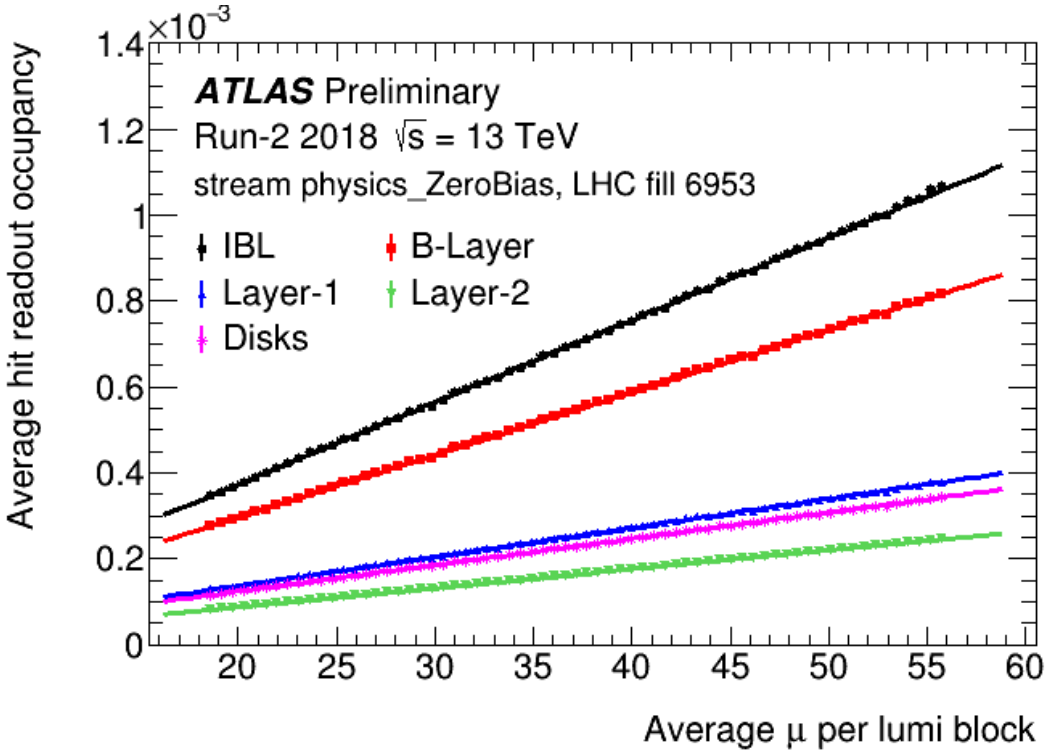

Operation in Run 2: Single Event Upsets

- Particles crossing the frontend chip can cause register settings to be corrupted.
- In IBL, the consequence of a global register upset is often visible as a drop in occupancy together with a change in current consumption. This is recoverable by reconfiguring the global registers.
- The global registers in the FEI4 are implemented as triple DICE latches. The main upset mechanism are glitches on the load line (SET).
- An automatic reconfiguration of the global registers inside a 2 ms gap every 5 seconds was implemented. Since this gap is without triggers, no deadtime is incurred.
- A pixel level reconfiguration will also be deployed.

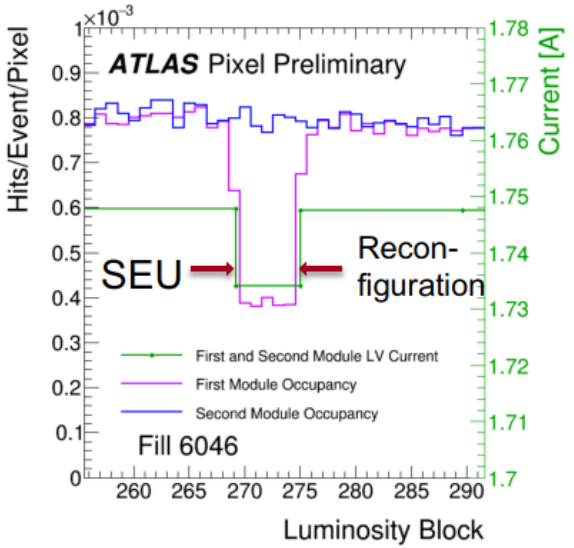

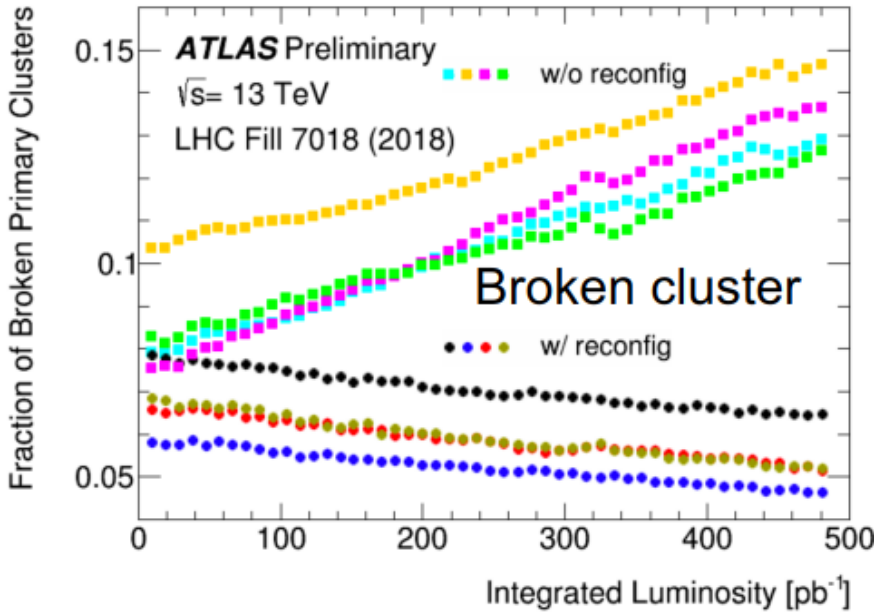

Operation in Run 2: IBL calibration drift

- The leakage currents inside the transistors of the FE-I4 readout chip (130 nm IBM process) show a strong dependence on TID with a peak at 1 Mrad.
- The leakage currents have a direct impact on the tuning of feedback currents and thresholds.
- The peak was overcome in 2016. Now we are on the falling edge.

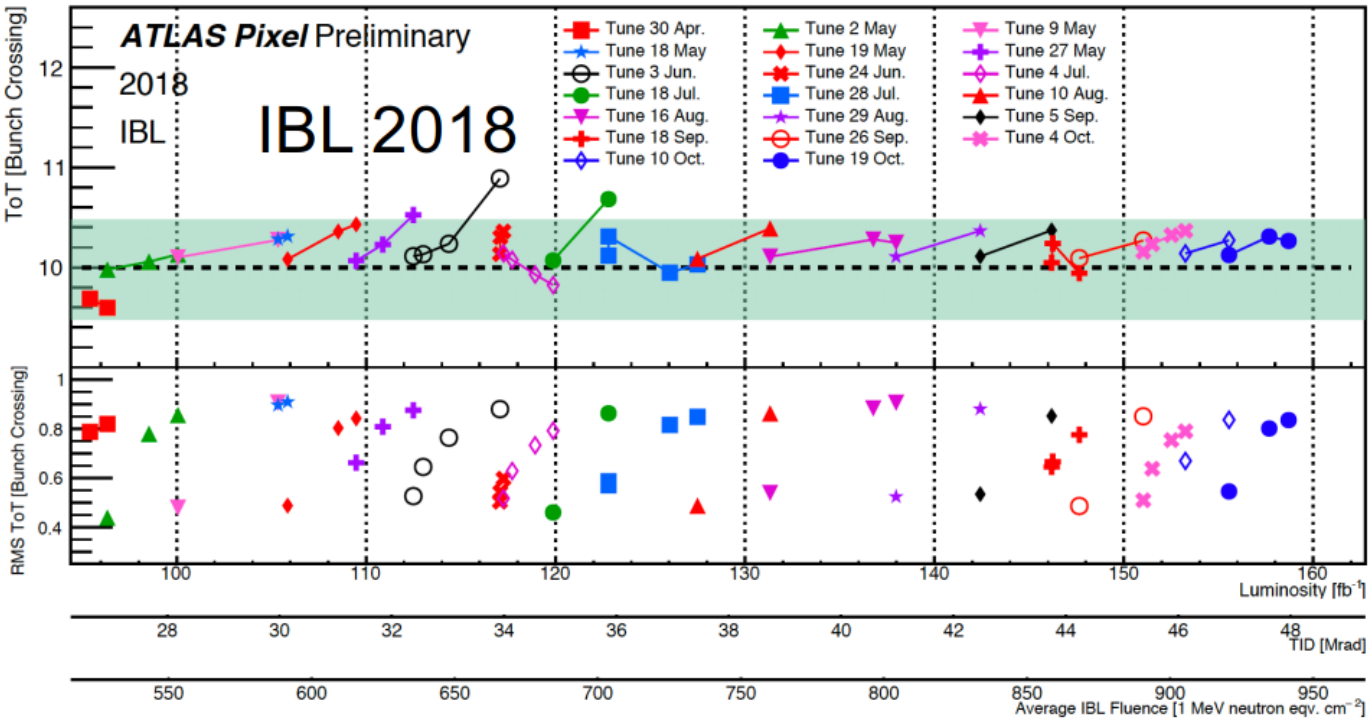

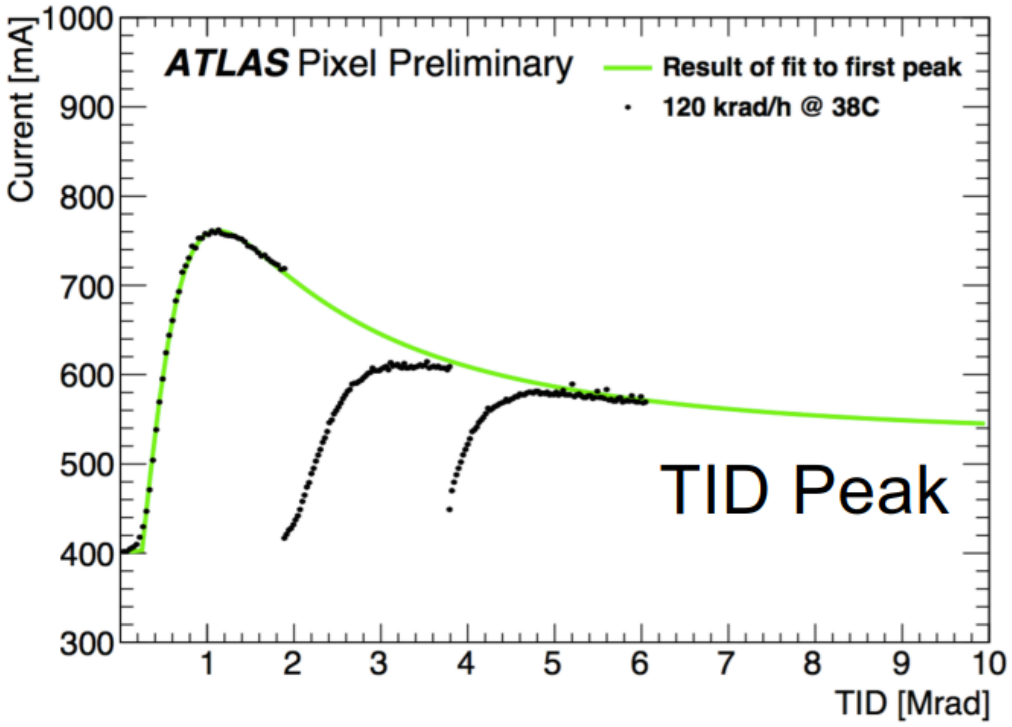

- The detuning of threshold and TOT is carefully monitored during LHC interfills.
- Depending on an appropriate window without beam for a retuning/recalibration.

Radiation Damage

- Radiation damage effects are getting to be significant for the performance of the detector.
- We expect a doubling of the accumulated luminosity during Run 3.
- Models are used to understand and predict radiation damage effects.
- The ATLAS Monte Carlo now includes radiation damage effects.
  - The new MC has been compared to earliest Run 3 data and demonstrated an overall good description of the pixel response.
- Some operational parameters (HV, thresholds, temperature) can be adjusted to counteract the effects.

Layer	End of Run 2 [neq cm^{-2}]	Limit [neq cm^{-2}]
IBL	$1x10^{15}$	$5x10^{15}$
B-Layer	$5x10^{14}$	$1x10^{15}$

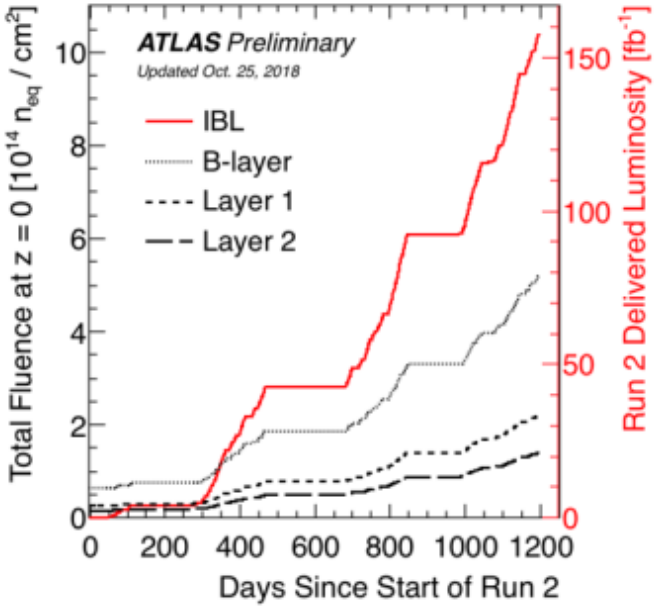

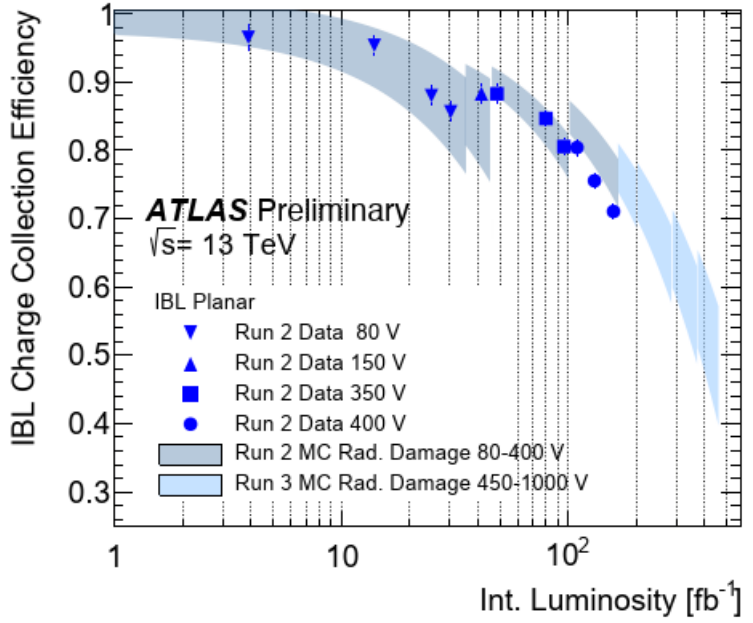

Depletion Voltage and Leakage Current

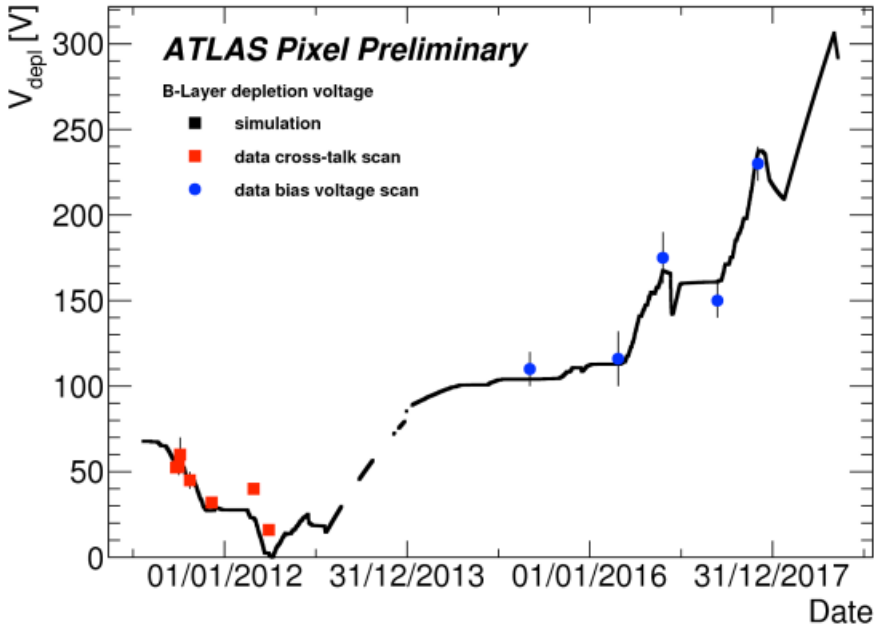

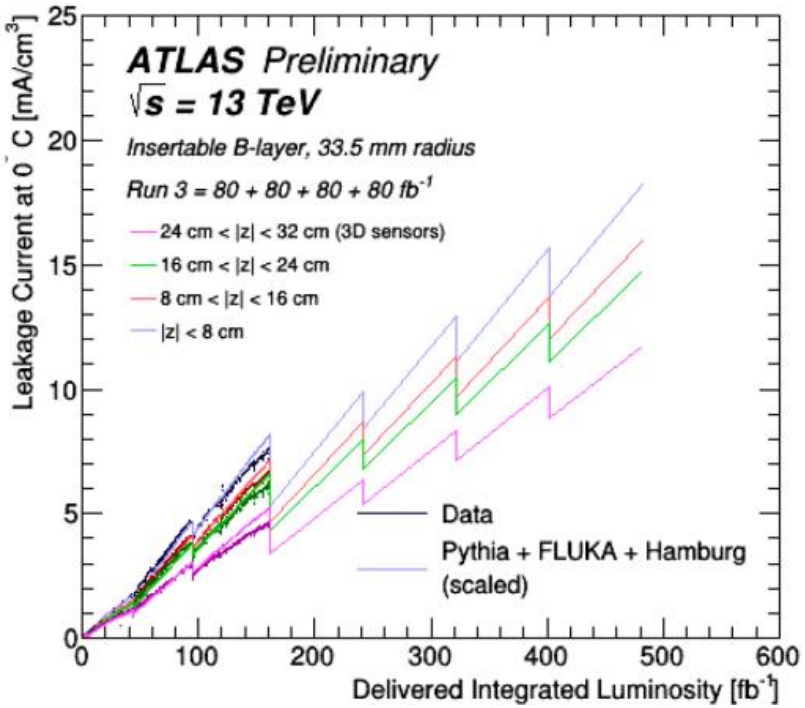

- Adjust **bias voltage** at the beginning of each year to guarantee a full depletion region for each year.
  - Depletion voltage is measured with data.
  - Data collected each year.
- At low fluences, the Hamburg model predictions and the data from the bias voltage scans were matched well.

- The evolution of the leakage current can be described with the Hamburg model. Global scaling factors are, however, required.
- Towards the end of run 2 the leakage current is overestimated.

Reverse Annealing

- Keeping the detector cold during the long shutdown was critical to prevent reverse annealing from driving the depletion voltage through the roof, in particular in B-layer and IBL.
  - This holds true also for operation during Run 3.
- There are hardware limitations for both bias voltage and leakage current.
- Warming up can not be completely avoided mainly due to required maintenance of the cooling system, but also in case access to the inside of the inner detector is needed, or unscheduled incidents (power cuts etc).
- The target during LS2 was to stay warm for less than 60 days during the shutdown.
- Detector was warm for 43 (23) days in Pixel (IBL).
- Multiple depletion voltage scans with cosmics ray data during LS2 indicate that annealing was minimal.

- *Pixel needs to be kept cold whenever possible*

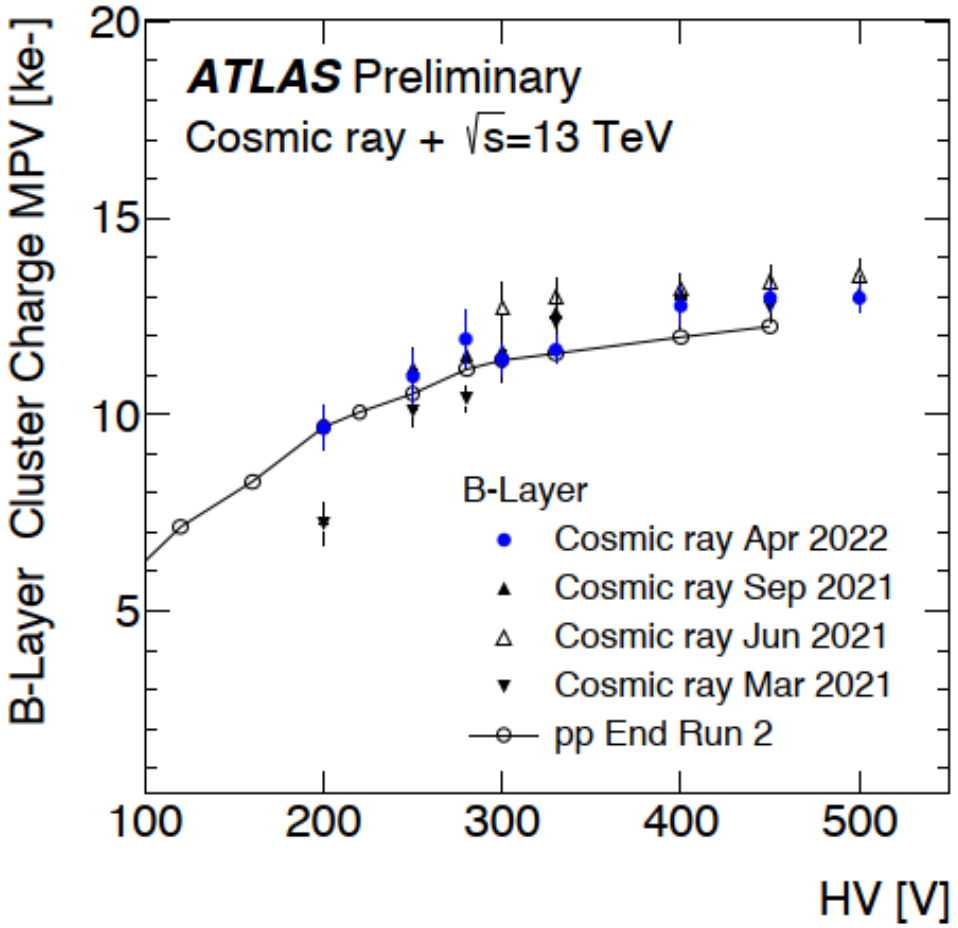

Lorentz Angle, dE/dx

Lorentz Angle

- Charges drift transversally in planar sensors because of the perpendicular magnetic field.
- The angle between electric field and the drift direction is called the Lorentz angle.
  - This effect introduces a bias on the cluster position reconstruction.
- The electric field changes with radiation damage. This results in a drift of the Lorentz angle with integrated luminosity.

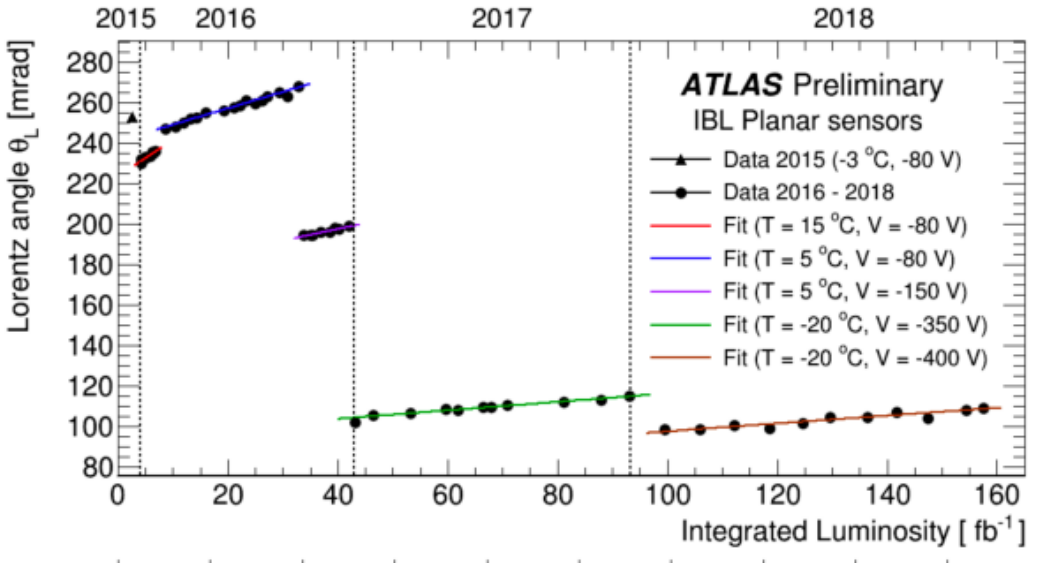

dE/dx

- Due to the decreasing charge collection efficiency the measured dE/dx decreases.
- Threshold changes show up as steps in dE/dx as well since hits below threshold do not get recorded.
- The HV can have an influence if the detector is not fully depleted.

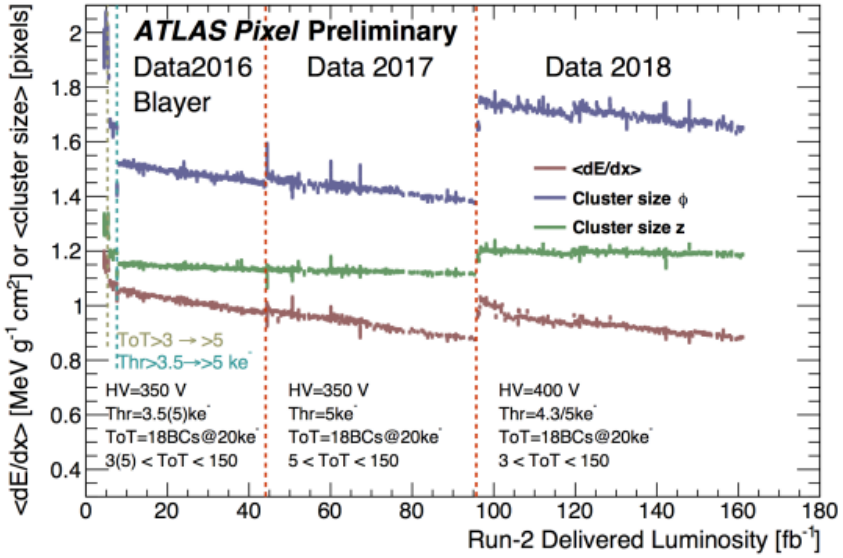

Threshold

- Occupancy decreases over time due to radiation damage causing efficiency losses.
- In 2018, the threshold could be lowered for the first time without hitting the bandwidth limitations, counteracting efficiency losses due to radiation damage.
- Optimization of keeping efficiency high and keeping the bandwidth manageable.

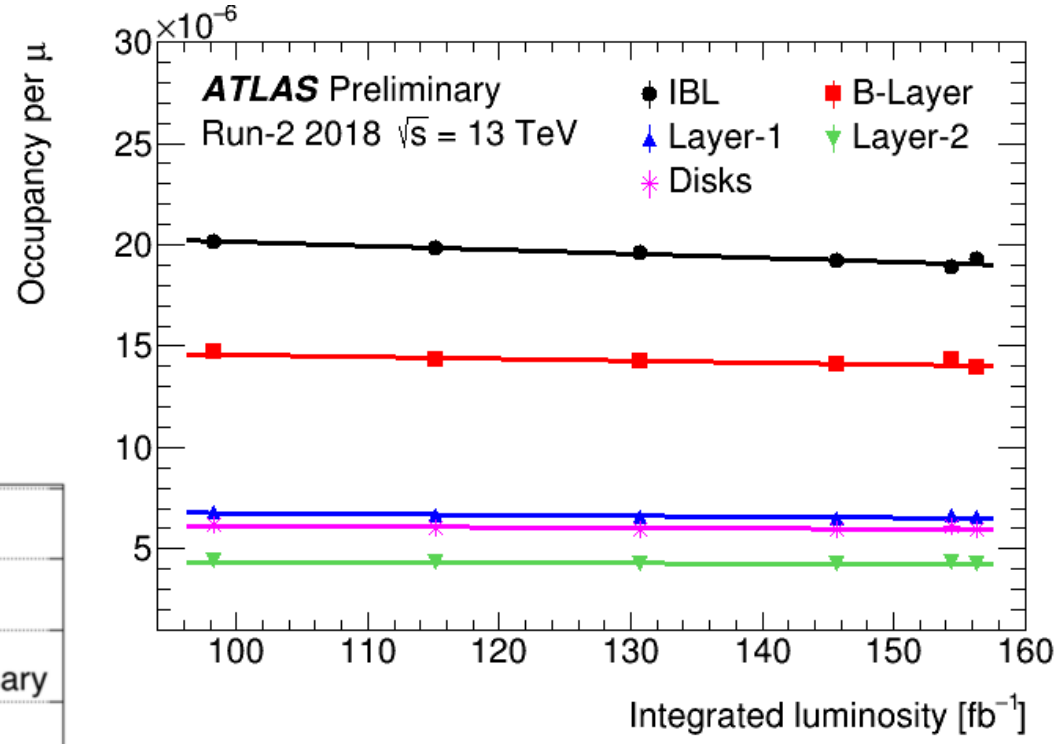

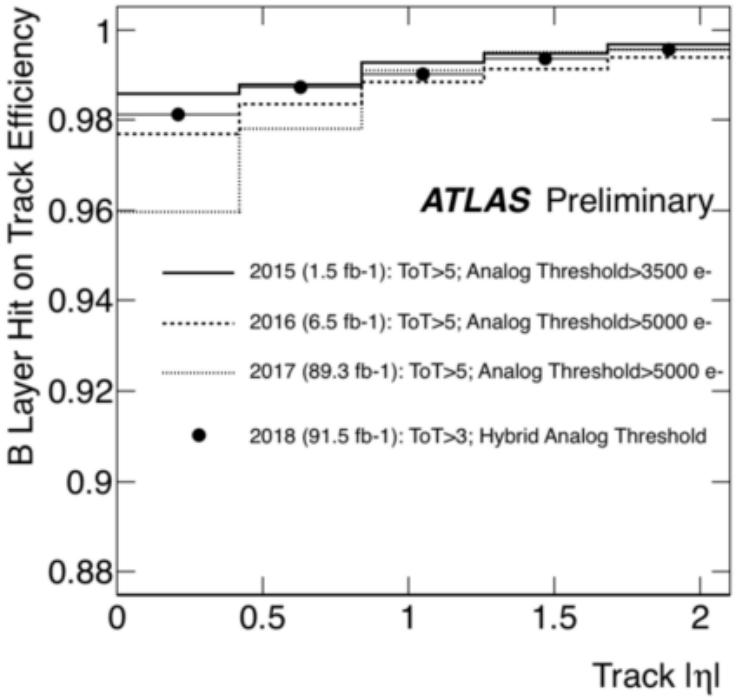

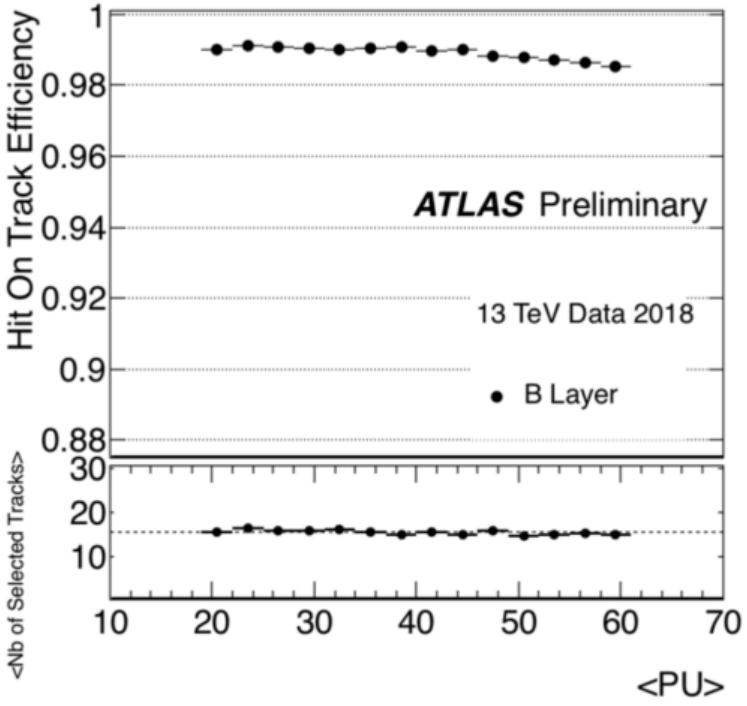

- Almost full efficiency in B-Layer recovered after lowering thresholds in 2018.
- Good stability of efficiency at high pile-up.

Optoboard replacement

- The major contribution to module failures during Run 2 was due to dark VCSEL channels.
- The failures started about 2 years after installation of the optoboards.
- Humidity is now the main suspect as failure cause.
- About 30 boards were replaced before the run of 2018. 20 additional VCSELs have died since then.
- An additional 400 optoboards were produced, and ca 2/3 of all optoboards were replaced during LS2, among them all failing and suspicious ones. In addition, the crates housing the optoboards were sealed against humidity.

- No new VCSEL channels have failed since then.

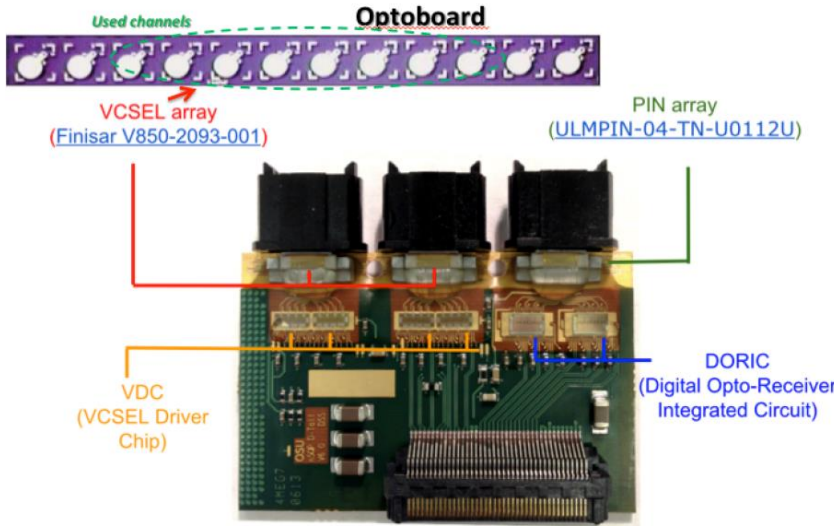

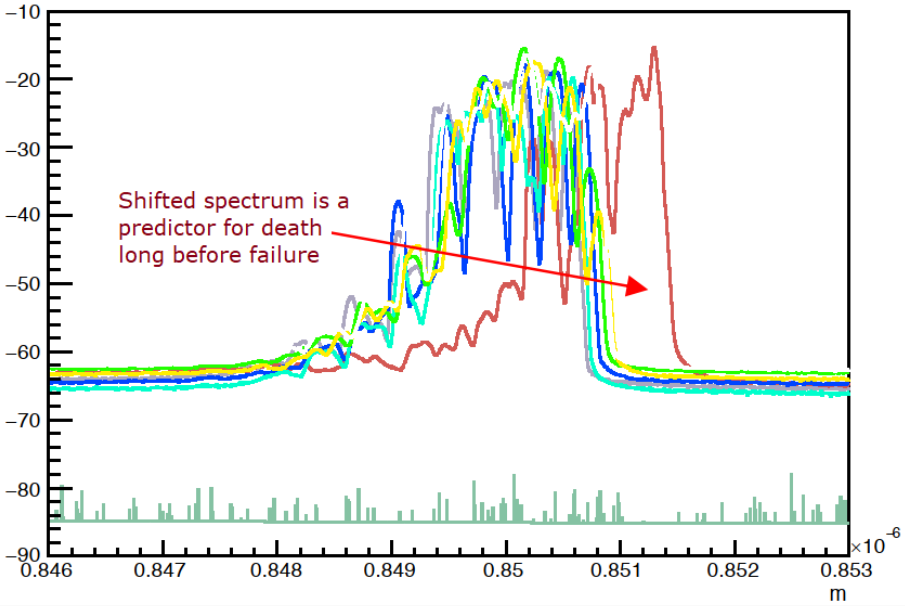

Long Shutdown 2

- The three years of LS2 were used to address weak points during Run 2 and to improve the system overall, e.g.
  - Streamlining the DAQ software for better maintainability and optimize usage of resources by the ROD firmware.
  - Optimize calibration procedures, to allow to go to even lower thresholds.
  - Tools for tracking detector behaviour, e.g. module failure types.
  - Better handling of missing hits in detector units (on the frontend level).
  - Development and implementation of a new Radiation Damage Digitizer in Monte Carlo, modelling the radiation damage to the Pixel sensors.
    - Signal is calculated using precise electric field, Lorentz angle and weighting potential maps, taking into account carriers trapping and diffusion effects.
      - Simulation of the electric field distribution for a given applied bias voltage after irradiation at a given fluence.
    - Now standard for Run 3 (all layers except IBL 3D and Pixel Disks due to performance constraints).
    - Exploit the radiation damage MC to train clustering/tracking algorithms.
    - Essential to understand and predict radiation damage effects and their relation to performance of physics object reconstruction.

LHC Startup 2022 (900 GeV)

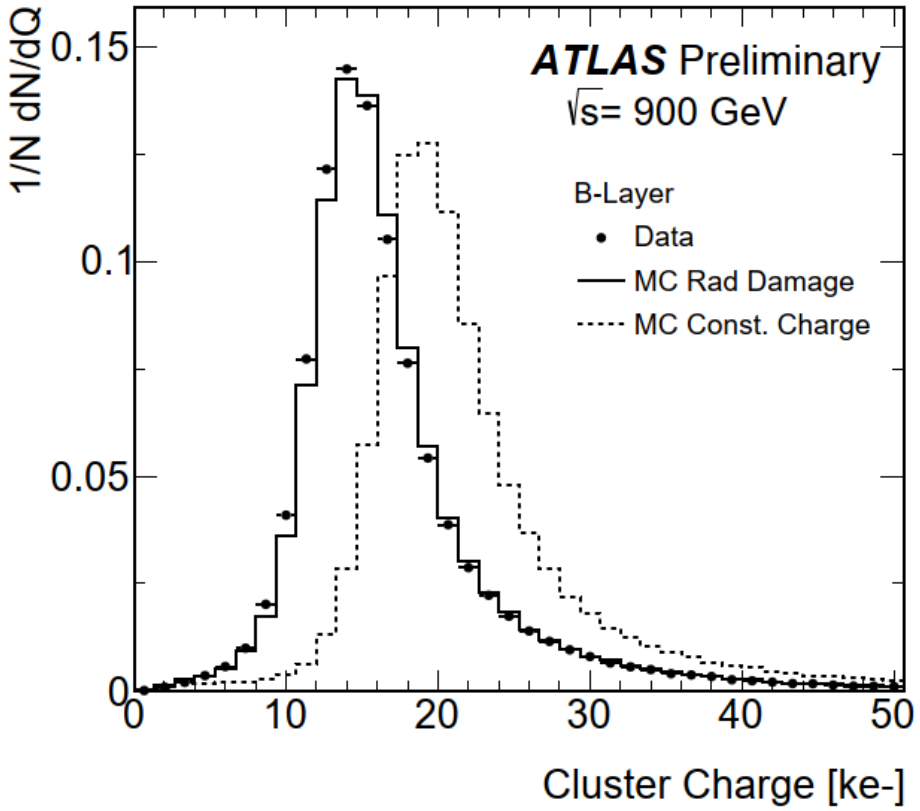

Effect of radiation damage on cluster charge data, well reproduced by new Radiation Damage MC.

- In the first half of the year, a large number of fills at injection energy (900 GeV) went into stable beams and were used for detector studies and tuning (timing, thresholds, HV).
- One of the most interesting uses was the early comparison of the new Radiation Damage Digitizer with data, both from the detector side and the performance (tracking) side with a very good synergy. Will exploit this also for early look at Run 3 performance.

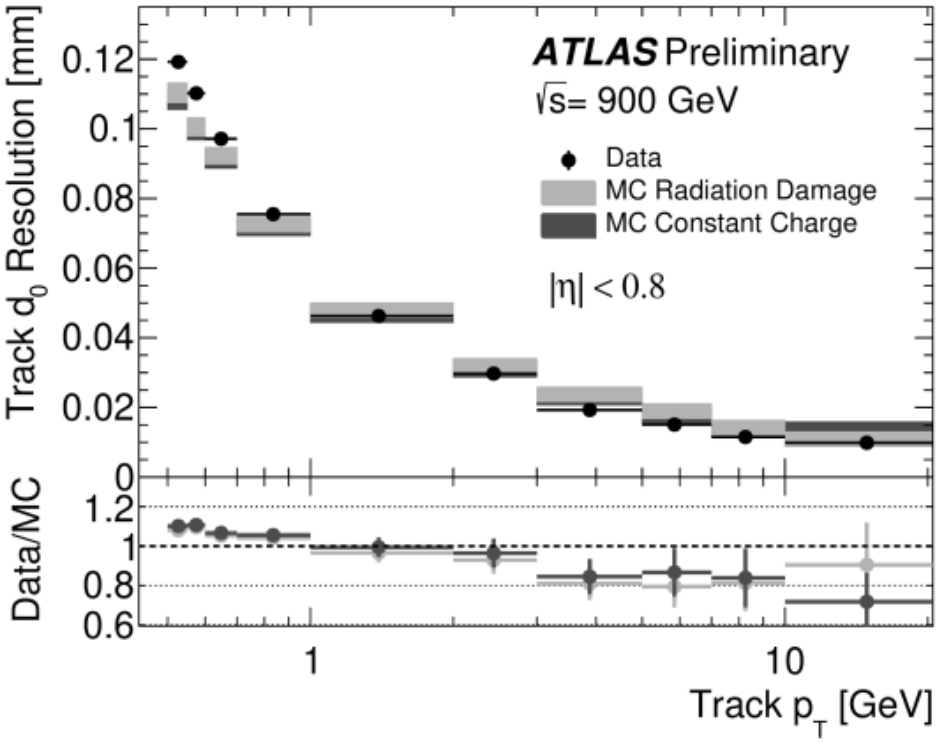

Spatial resolution is well reproduced by new Radiation Damage MC. For the Run 2 fluence, there is only a limited effect on the tracking performance: impact parameter d_0 resolution well reproduced by both MC.

Conclusion and Outlook

- The ATLAS Pixel detector has delivered excellent performance in Run 2, even though radiation damage is becoming very noticeable. Much learned from operation in Run 2.
- The operational parameters have to be retuned to guarantee optimal data quality and efficiency. Further decrease in threshold for the start of Run 3, keeping inside predicted bandwidth expectations.
- LHC was in shutdown for three years. For Pixel the biggest hardware project was the successful replacement of the optical data transmitters on the detector. After sealing them against humidity, no further failures have been observed.
- On the software side, many improvements were implemented during LS2, but for the final validation often realistic beam conditions are needed. Many of these updates are now improving operation, and the Pixel Detector is running stably. Further work to re-optimize the performance is planned.
- Aging hardware is generally a concern, situation and availability of spares needs to be closely monitored.
- The main concern is the accumulating radiation damage. Trying on the one side to mitigate the effects themselves by tuning and optimising operational parameters, and on the other side by predicting its effects in simulation and taking them into account in data reconstruction.

- We are approaching the end of the first year of Run 3, with the Pixel Detector running stably but further improvements and understanding of the Run 3 data taking conditions to be addressed.
- Then we have three more years of running in Run 3, with Radiation damage the main concern.

BACKUP

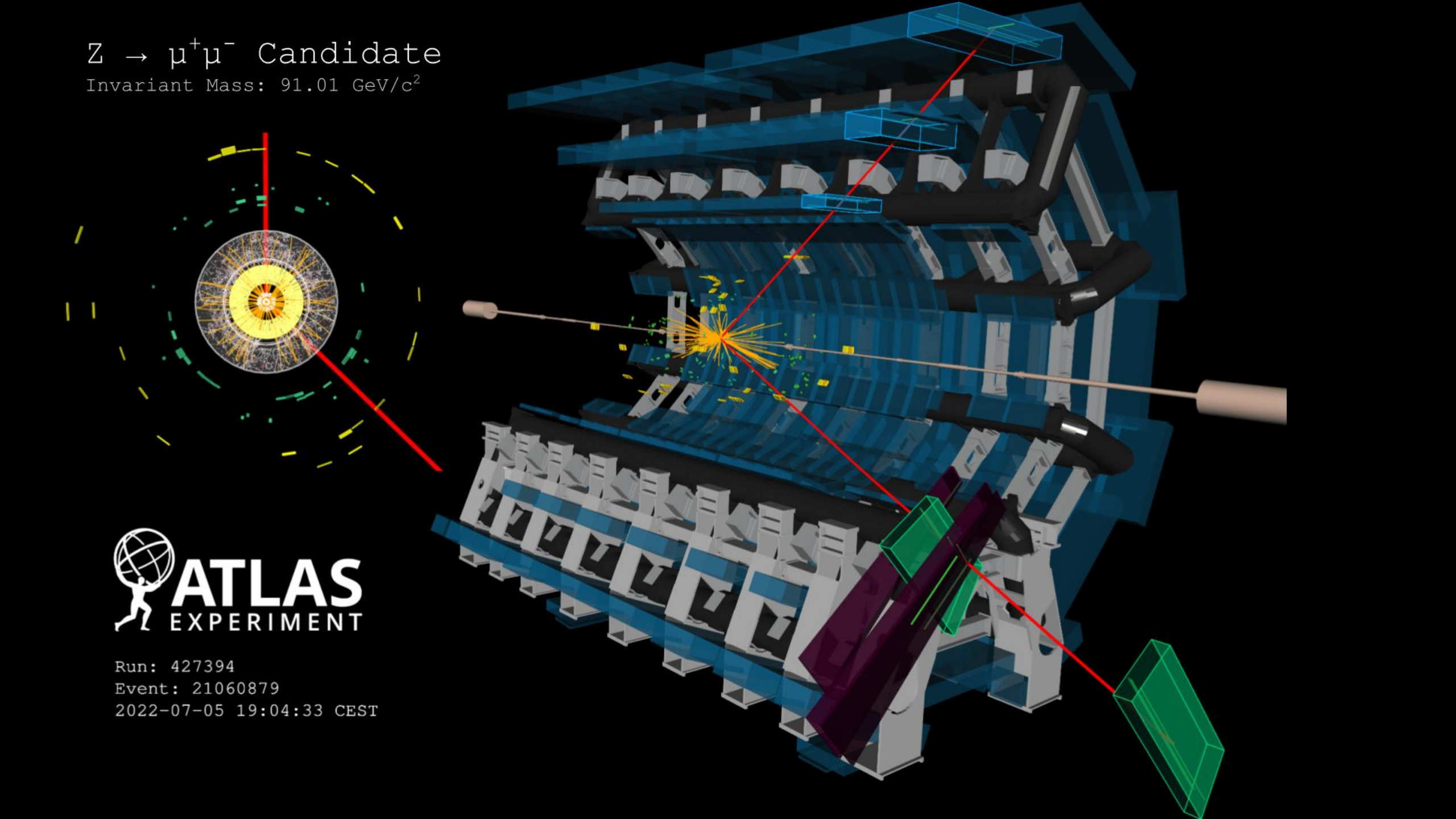
Z → μ⁺μ⁻ Candidate
Invariant Mass: 91.01 GeV/c²
ATLAS
EXPERIMENT
Run: 427394
Event: 21060879
2022-07-05 19:04:33 CEST

Desynchronisation

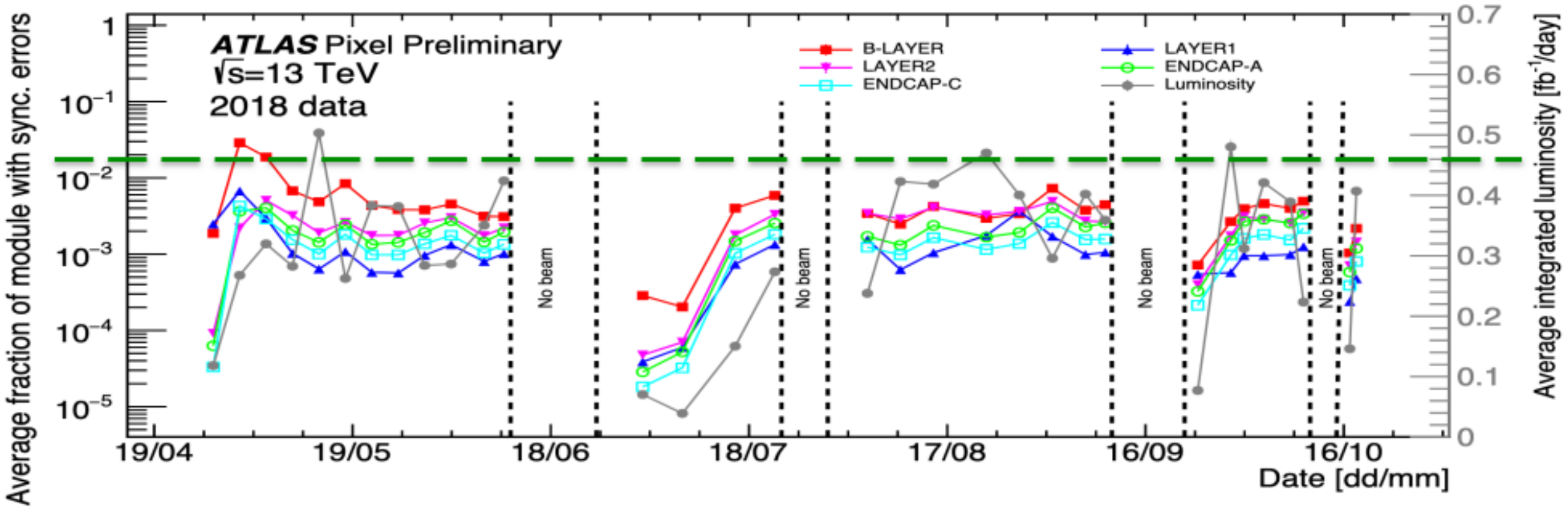

IBL SEU

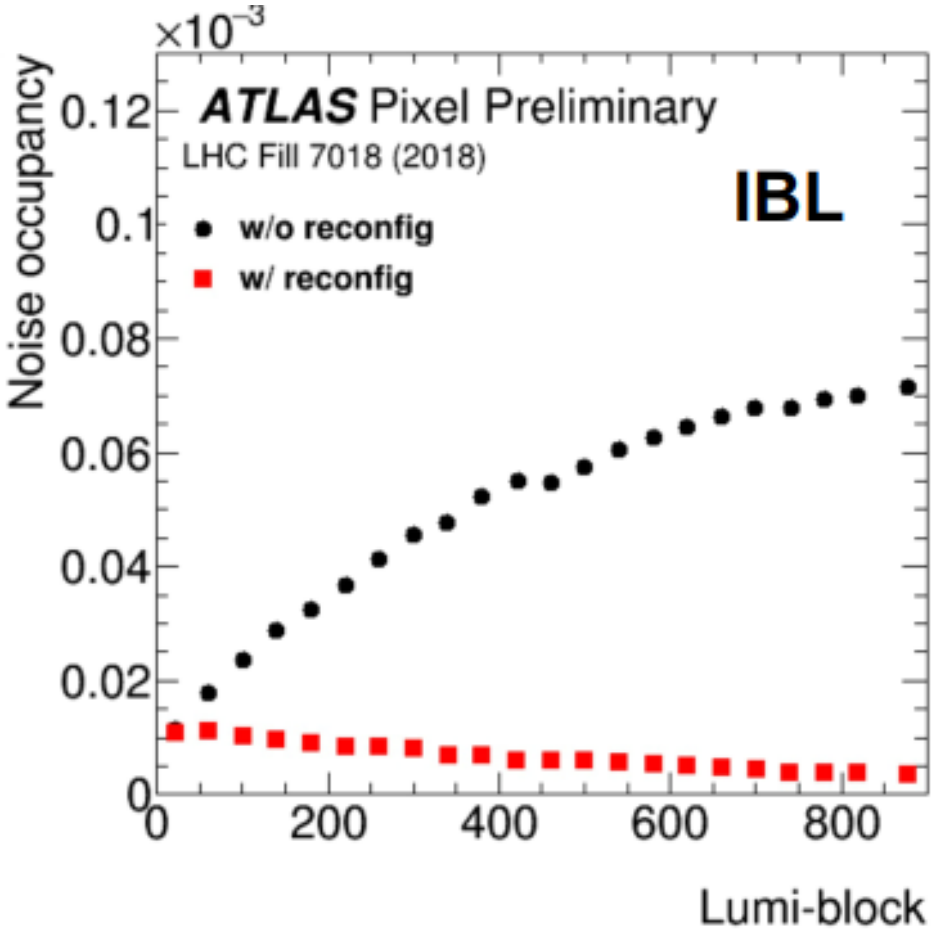
×10⁻³
Noise occupancy
0.12
0.1
0.08
0.06
0.04
0.02
0
ATLAS Pixel Preliminary
LHC Fill 7018 (2018)
IBL
w/o reconfig
w/ reconfig
0
200
400
600
800
Lumi-block

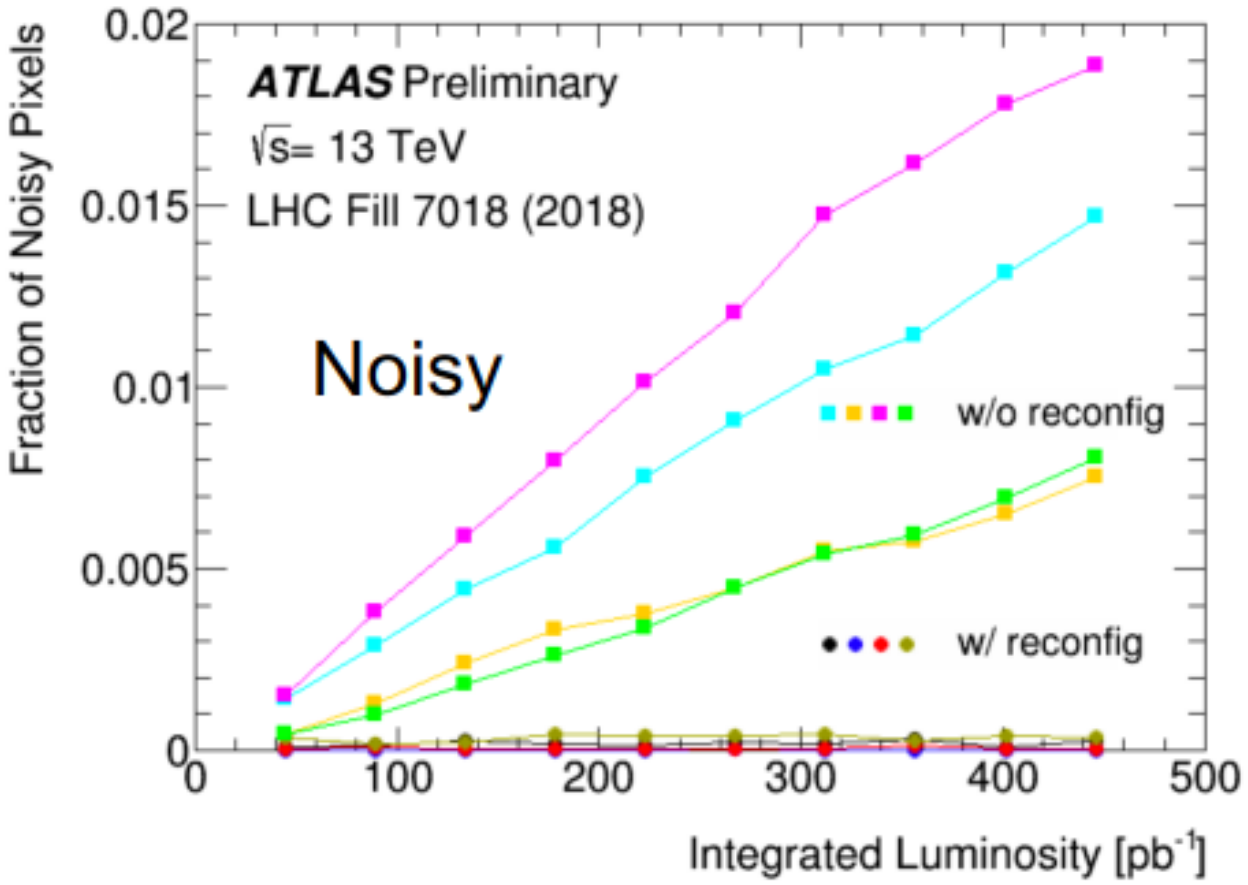
Fraction of Noisy Pixels
0.02
0.015
0.01
0.005
0
ATLAS Preliminary
√s= 13 TeV
LHC Fill 7018 (2018)
Noisy
w/o reconfig
w/ reconfig
0
100
200
300
400
500
Integrated Luminosity [pb⁻¹]

Pixel Leakage Current

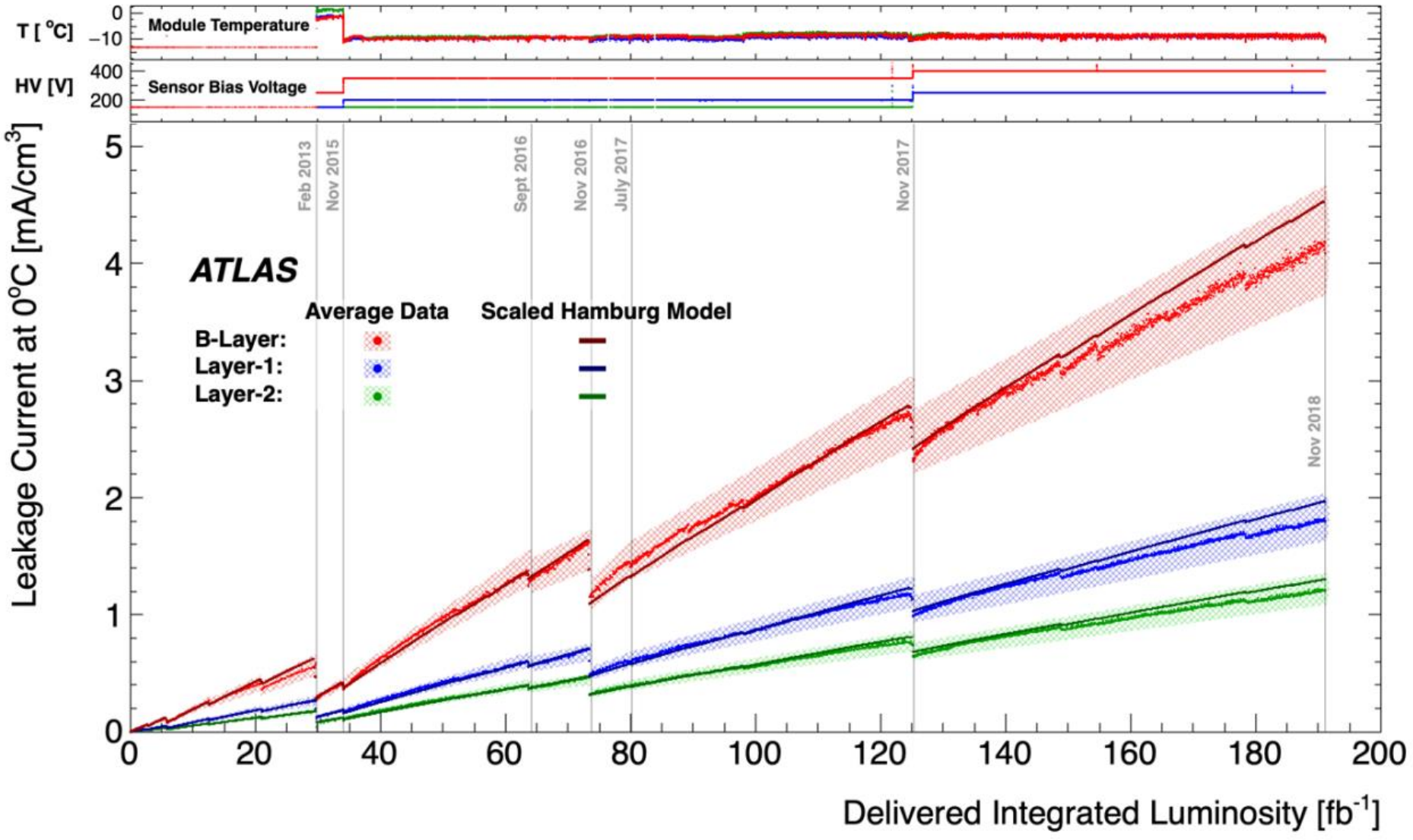

IBL dE/dx

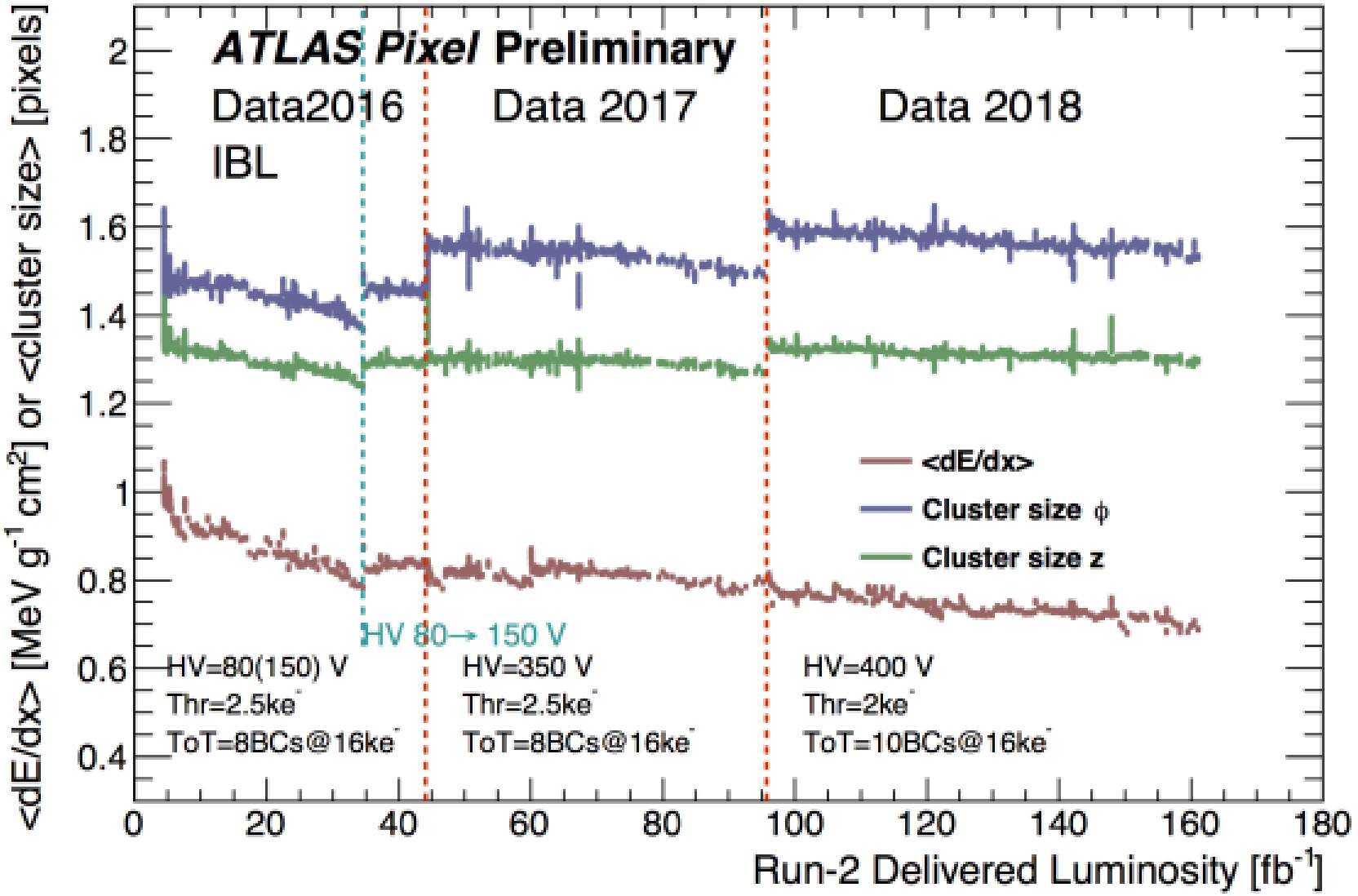
ATLAS Pixel Preliminary
Data2016
Data 2017
Data 2018
IBL
<dE/dx>
Cluster size ϕ
Cluster size z
HV 80→ 150 V
HV=80(150) V
Thr=2.5ke⁻
ToT=8BCs@16ke⁻
HV=350 V
Thr=2.5ke⁻
ToT=8BCs@16ke⁻
HV=400 V
Thr=2ke⁻
ToT=10BCs@16ke⁻
<dE/dx> [MeV g⁻¹ cm²] or <cluster size> [pixels]
Run-2 Delivered Luminosity [fb⁻¹]
0.4
0.6
0.8
1
1.2
1.4
1.6
1.8
2
0
20
40
60
80
100
120
140
160
180

Fluence vs z

- Comparison of simulated fluence with the fluence obtained from the leakage currents using the Hamburg model.
- Simulated fluence for Pixel slightly below leakage current fluence.
- IBL simulated fluence quite flat along z. The leakage current fluence has a strong z dependence.
- The z dependence is also observed in the depletion voltage.

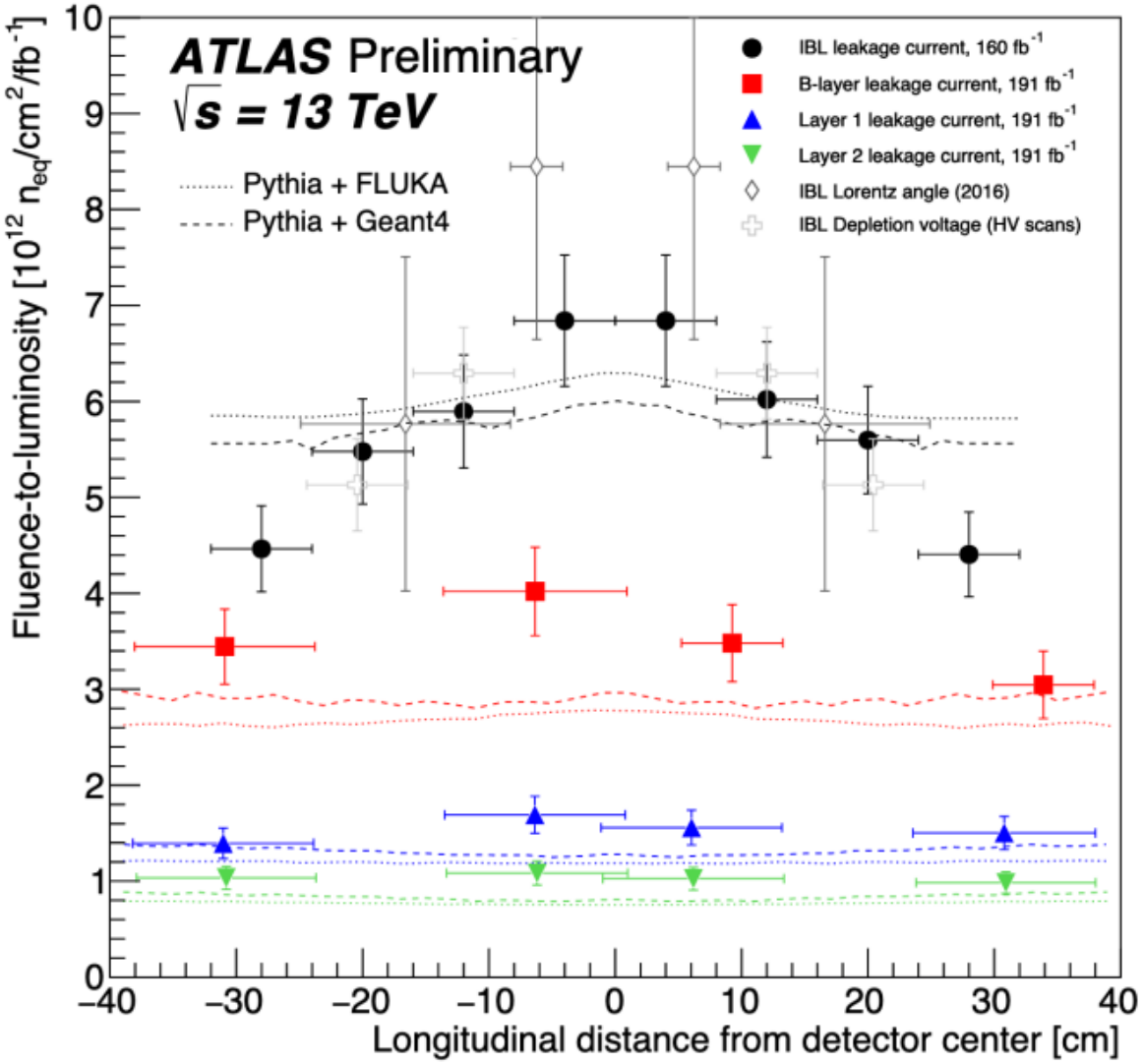

LHC longterm schedule

- Run 1:
  - 2011 (3.5 TeV)
  - 2012 (4 TeV)

  ---------- LS1: 2013-15 ----------
- Run 2 (6.5 TeV)
  - 2015
  - 2016
  - 2017
  - 2018

  ---------- LS2: 2019-22 ----------
- Run 3 (6.8 TeV) foreseen
  - 2022
  - 2023
  - 2024
  - 2025

Radiation Damage MC vs 900 GeV

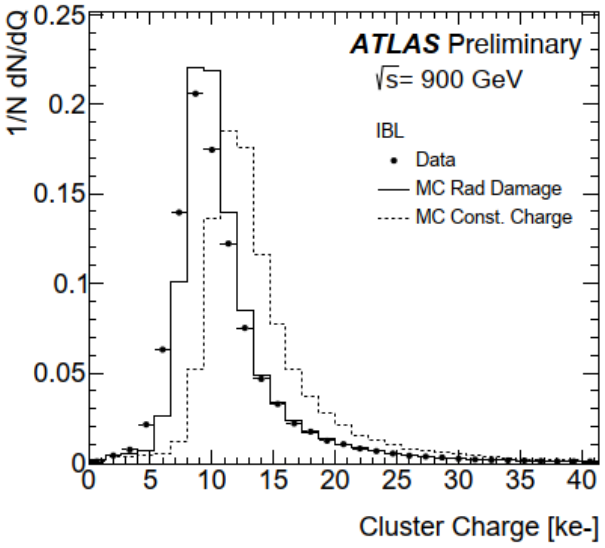

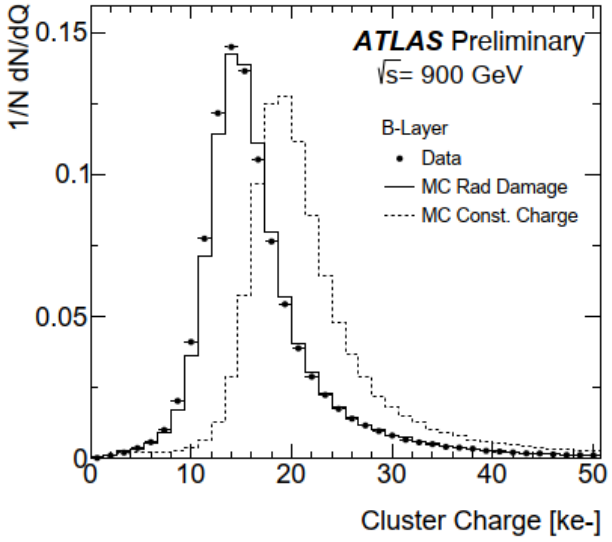

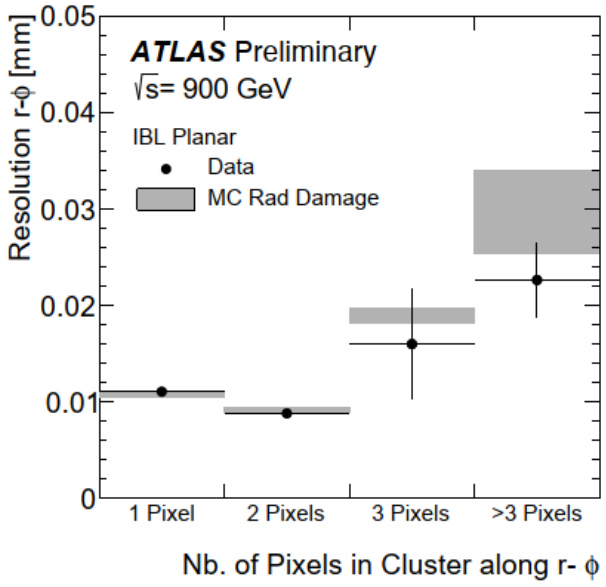

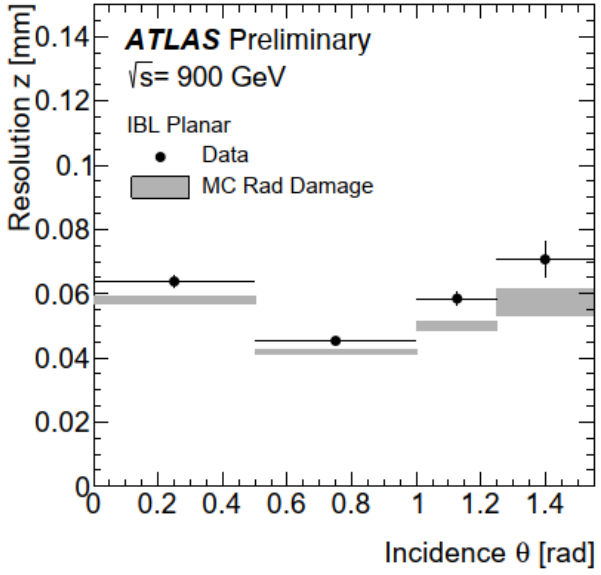

2022

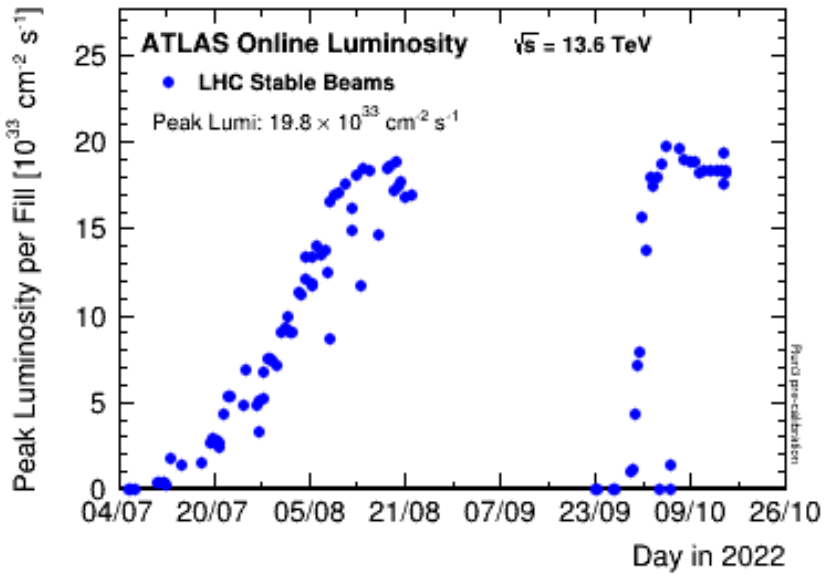
ATLAS Online Luminosity
√s = 13.6 TeV
LHC Stable Beams
Peak Lumi: 19.8 × 10^33 cm^-2 s^-1
Peak Luminosity per Fill [10^33 cm^-2 s^-1]
0
5
10
15
20
25
04/07
20/07
05/08
21/08
07/09
23/09
09/10
26/10
Day in 2022

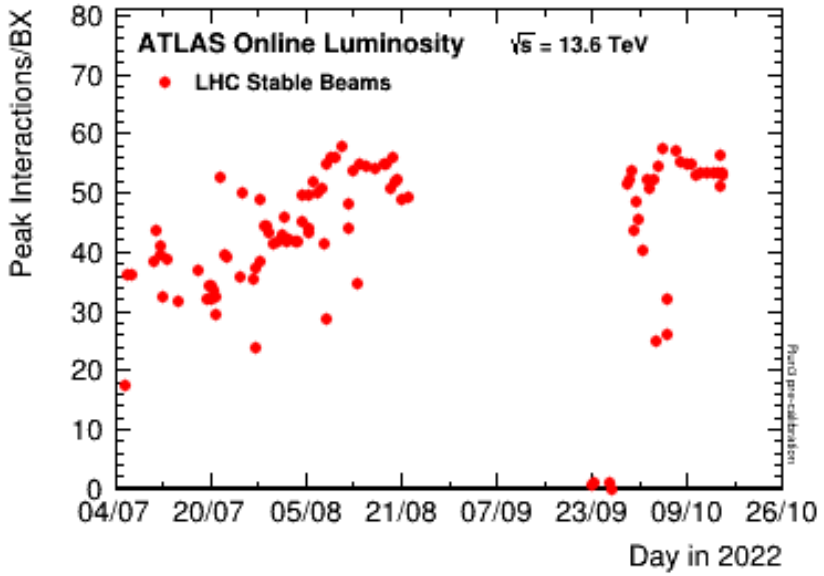
ATLAS Online Luminosity
√s = 13.6 TeV
LHC Stable Beams
Peak Interactions/BX
0
10
20
30
40
50
60
70
80
04/07
20/07
05/08
21/08
07/09
23/09
09/10
26/10
Day in 2022

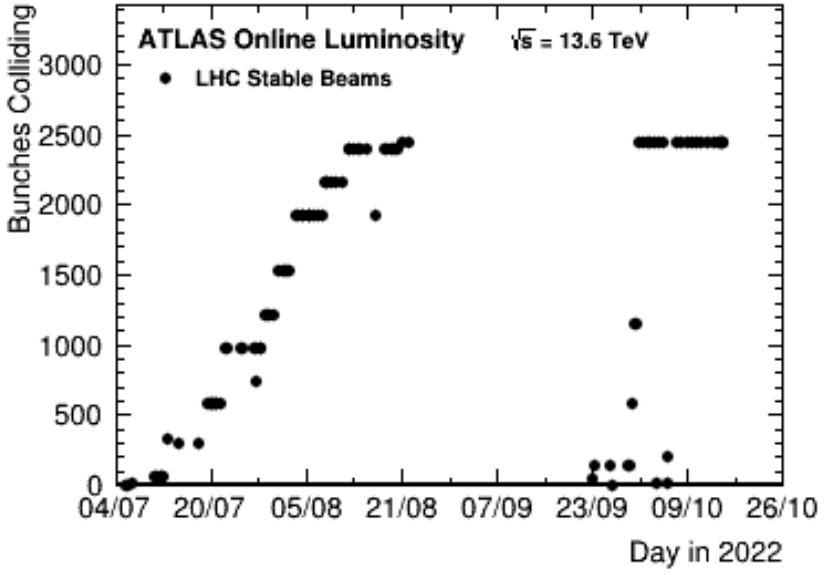
ATLAS Online Luminosity
√s = 13.6 TeV
LHC Stable Beams
Bunches Colliding
0
500
1000
1500
2000
2500
3000
04/07
20/07
05/08
21/08
07/09
23/09
09/10
26/10
Day in 2022

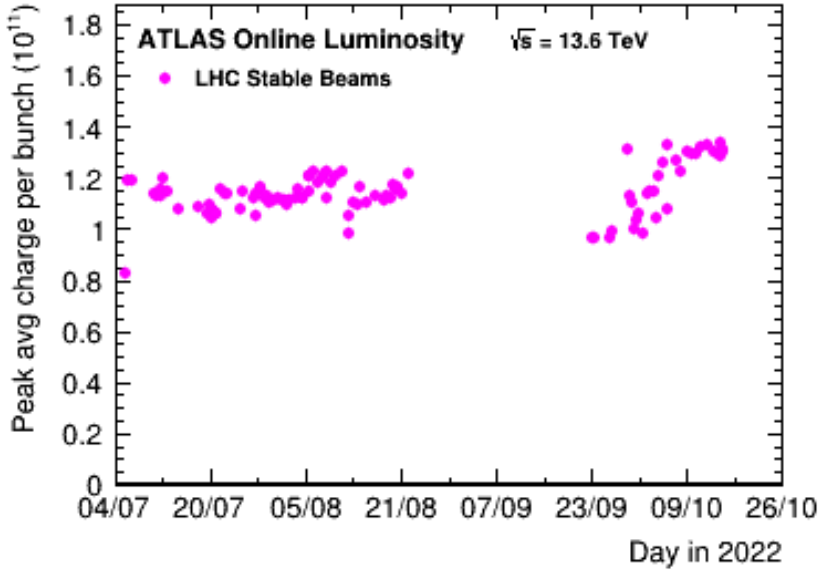
ATLAS Online Luminosity
√s = 13.6 TeV
LHC Stable Beams
Peak avg charge per bunch (10^11)
0
0.2
0.4
0.6
0.8
1
1.2
1.4
1.6
1.8
04/07
20/07
05/08
21/08
07/09
23/09
09/10
26/10
Day in 2022

2018

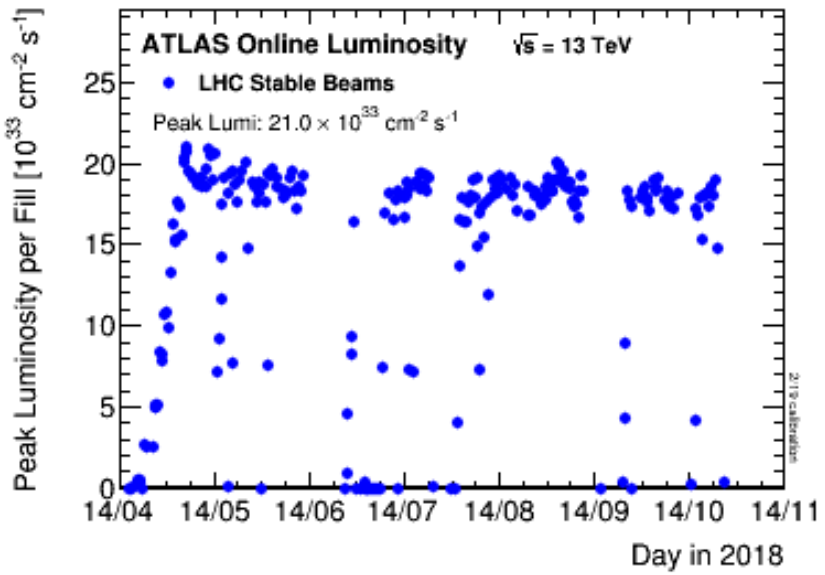
ATLAS Online Luminosity
√s = 13 TeV
LHC Stable Beams
Peak Lumi: 21.0 × 10^33 cm^-2 s^-1
Peak Luminosity per Fill [10^33 cm^-2 s^-1]
Day in 2018

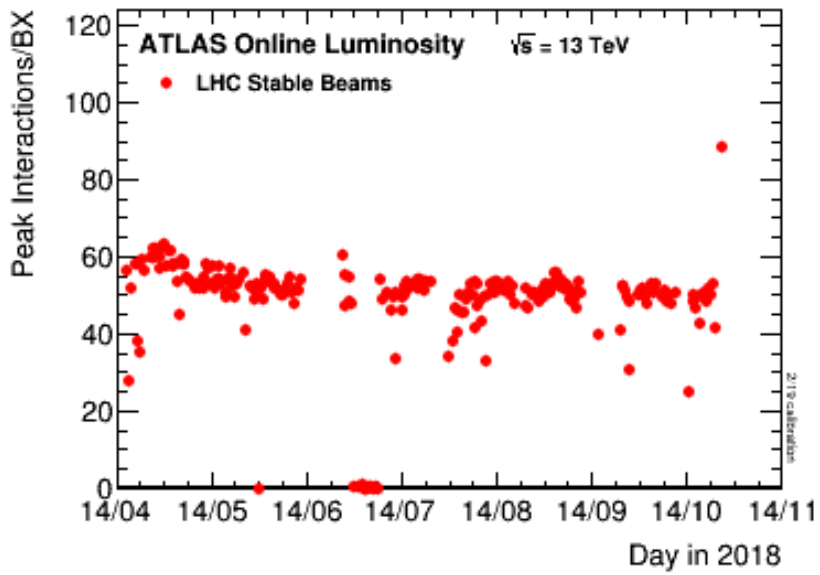
ATLAS Online Luminosity
√s = 13 TeV
LHC Stable Beams
Peak Interactions/BX
Day in 2018

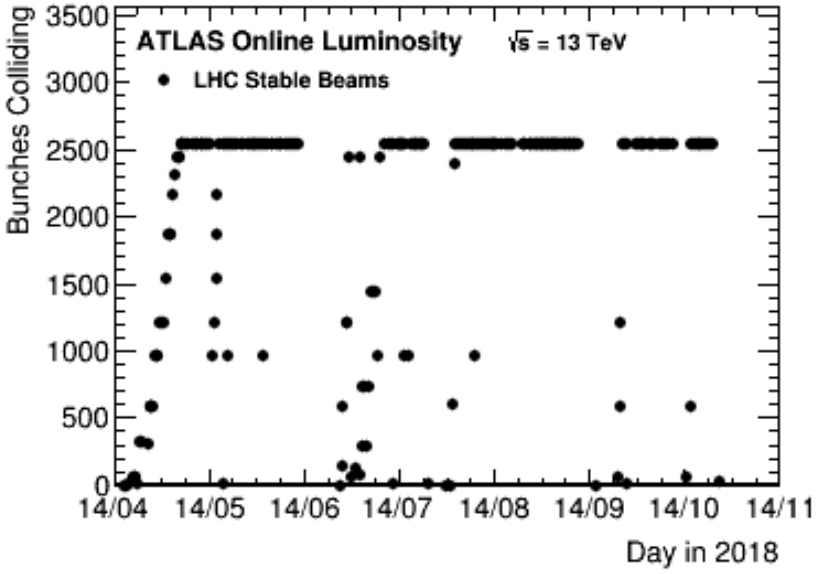
ATLAS Online Luminosity
√s = 13 TeV
LHC Stable Beams
Bunches Colliding
Day in 2018

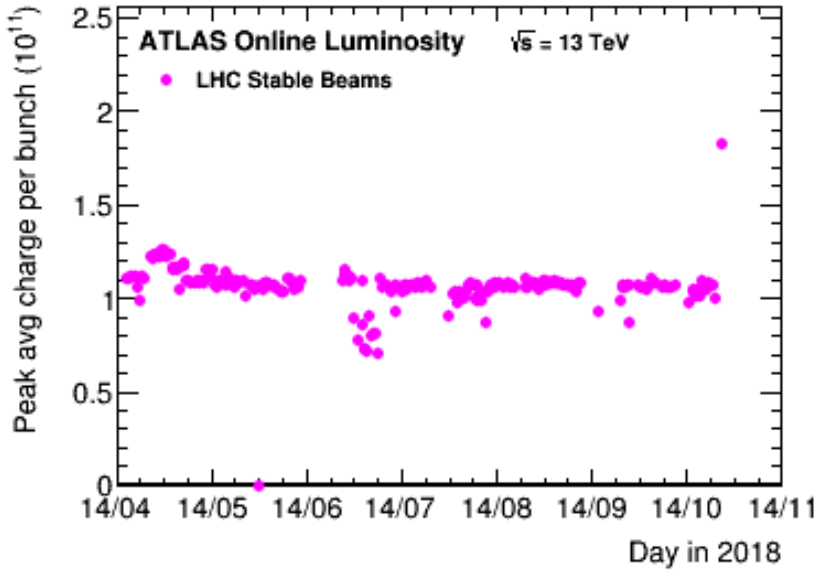
ATLAS Online Luminosity
√s = 13 TeV
LHC Stable Beams
Peak avg charge per bunch (10^11)
Day in 2018

2017

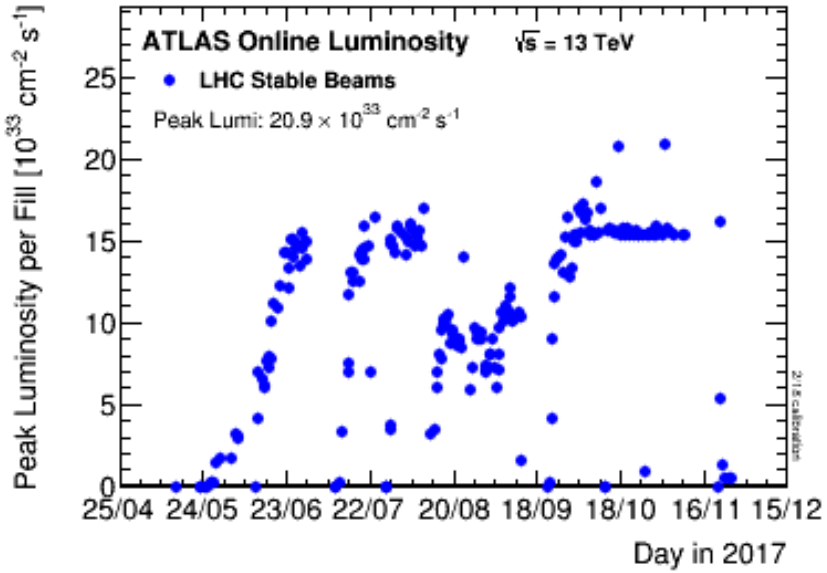
ATLAS Online Luminosity
√s = 13 TeV
LHC Stable Beams
Peak Lumi: 20.9 × 10^33 cm^-2 s^-1
Peak Luminosity per Fill [10^33 cm^-2 s^-1]
25/04 24/05 23/06 22/07 20/08 18/09 18/10 16/11 15/12
Day in 2017

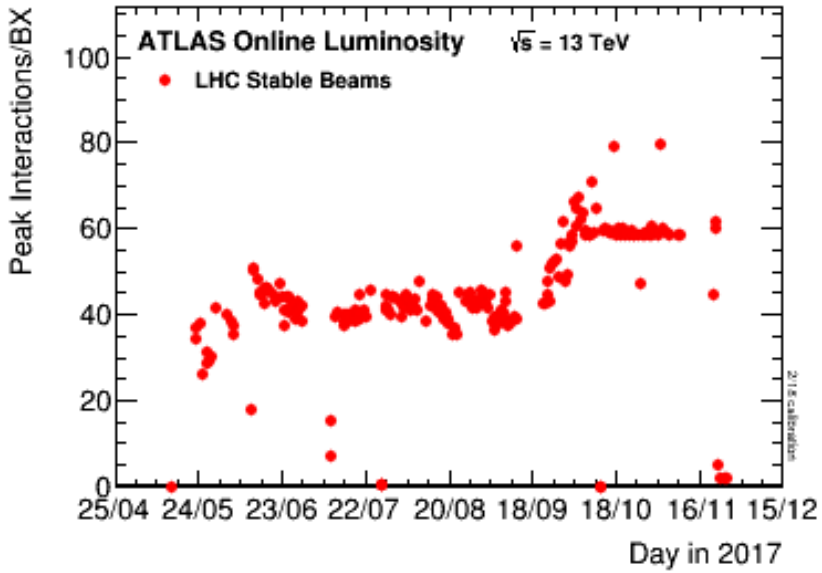
ATLAS Online Luminosity
√s = 13 TeV
LHC Stable Beams
Peak Interactions/BX
25/04 24/05 23/06 22/07 20/08 18/09 18/10 16/11 15/12
Day in 2017

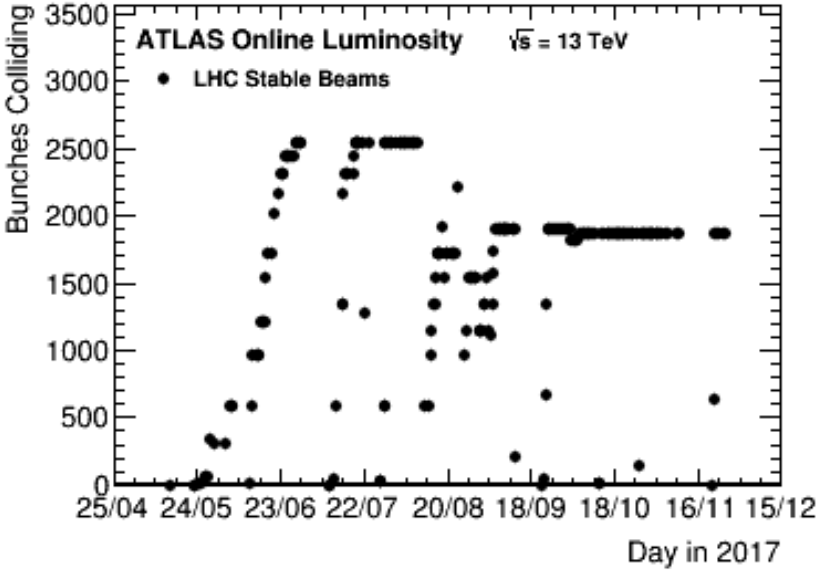
ATLAS Online Luminosity
√s = 13 TeV
LHC Stable Beams
Bunches Colliding
25/04 24/05 23/06 22/07 20/08 18/09 18/10 16/11 15/12
Day in 2017

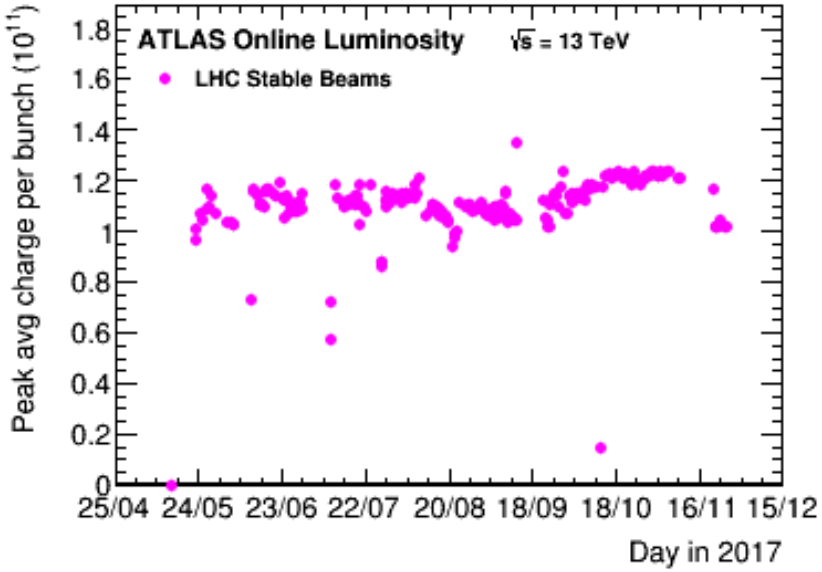
ATLAS Online Luminosity
√s = 13 TeV
LHC Stable Beams
Peak avg charge per bunch (10^11)
25/04 24/05 23/06 22/07 20/08 18/09 18/10 16/11 15/12
Day in 2017

2016

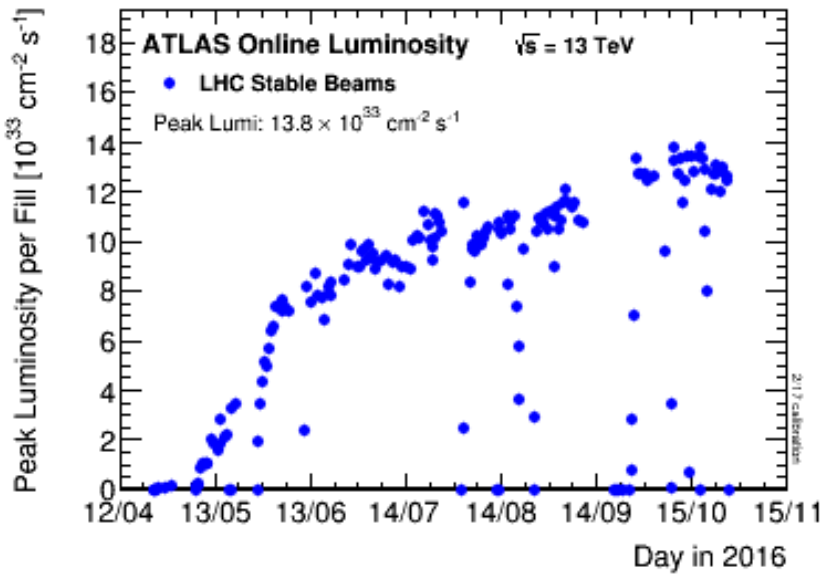
ATLAS Online Luminosity
√s = 13 TeV
LHC Stable Beams
Peak Lumi: 13.8 × 10^33 cm^-2 s^-1
Peak Luminosity per Fill [10^33 cm^-2 s^-1]
Day in 2016

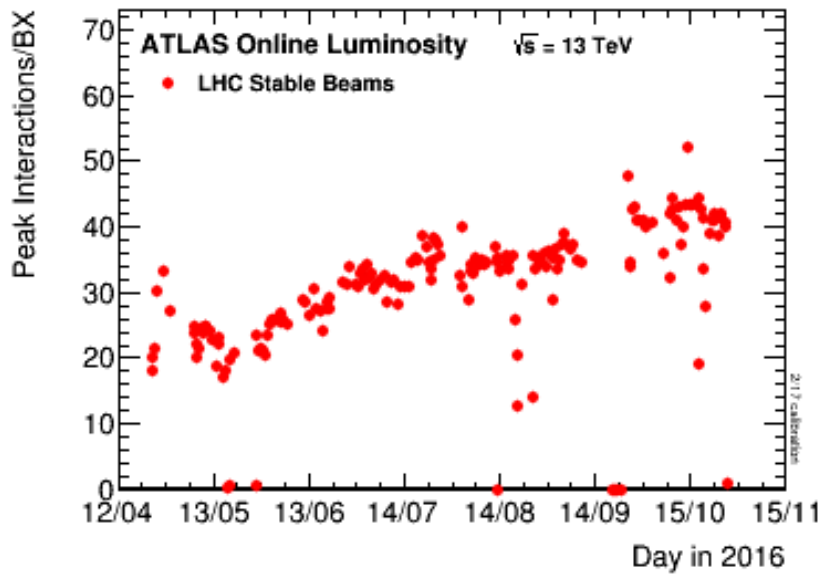
ATLAS Online Luminosity
√s = 13 TeV
LHC Stable Beams
Peak Interactions/BX
Day in 2016

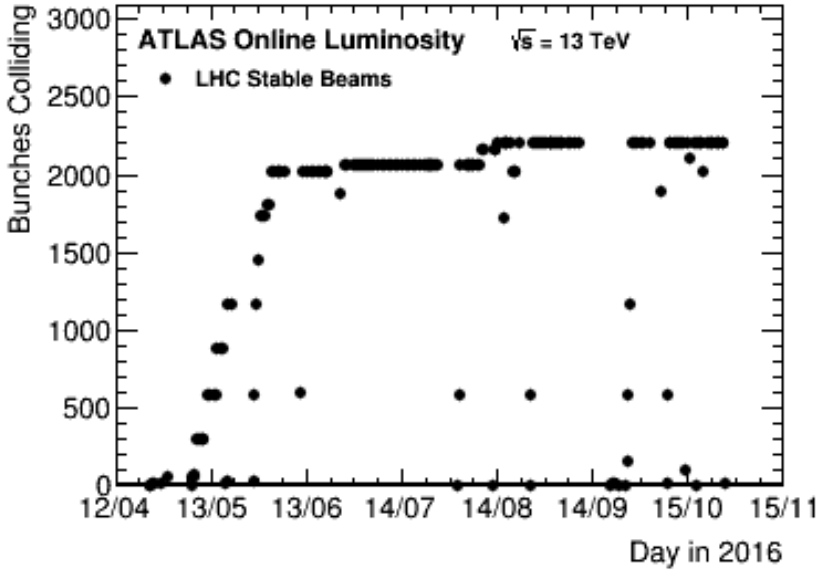
ATLAS Online Luminosity
√s = 13 TeV
LHC Stable Beams
Bunches Colliding
Day in 2016

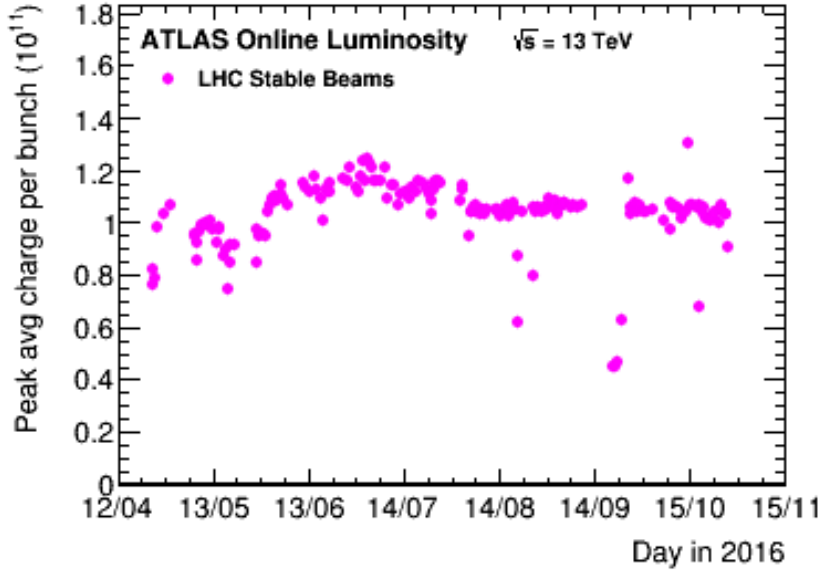
ATLAS Online Luminosity
√s = 13 TeV
LHC Stable Beams
Peak avg charge per bunch (10^11)
Day in 2016